Dark matter effective field theory and an application to vector dark matter

Jason Aebischer,[a] **Wolfgang Altmannshofer,**[b] **Elizabeth E. Jenkins**[c] **and Aneesh V. Manohar**[c]

[a]*Physik-Institut, Universität Zürich,*
Winterthurerstrasse 190, CH-8057 Zürich, Switzerland

[b]*Department of Physics and Santa Cruz Institute for Particle Physics, University of California,*
1156 High St, Santa Cruz, CA 95064, U.S.A.

[c]*Department of Physics, University of California,*
San Diego, 9500 Gilman Drive, La Jolla, CA 92093-0319, U.S.A.

E-mail: jason.aebischer@physik.uzh.ch, waltmann@ucsc.edu,
ejenkins@ucsd.edu, amanohar@ucsd.edu

Abstract: The Standard Model Effective Field Theory (SMEFT) and the Low Energy Effective Field Theory (LEFT) can be extended by adding additional spin 0, 1/2 and 1 dark matter particles which are singlets under the Standard Model (SM) gauge group. We classify all gauge invariant interactions in the Lagrangian up to terms of dimension six, and present the tree-level matching conditions between the two theories at the electroweak scale. The most widely studied dark matter models, such as those based on the Higgs portal or on kinetic mixing between the photon and a dark photon, are based on dimension-four interactions with the SM sector. We consider a model with dark vector particles with a $\mathbb{Z}_2$ symmetry, so that the lightest dark matter particle is stable. The leading interaction with the SM is through dimension-six operators involving two dark vector field-strength tensors and the electromagnetic field-strength tensor. This model is a viable dark matter model in the freeze-in scenario for a wide range of parameters.

Contents

1 Introduction

Dark Matter (DM) is a viable candidate to explain a number of otherwise unexplained observations in the universe. Evidence for dark matter is astrophysical or cosmological — galactic rotation curves, gravitational lensing, the cosmic microwave background fluctuations, large scale structure, etc.

Particle physics explanations for DM add one or more new particles which interact weakly with the Standard Model (SM) particles. To study the implications of additional DM particles in a model-independent way, it is convenient to adopt an Effective Field Theory (EFT) approach. A DM EFT (DMEFT) consists of local operators constructed from SM as well as DM fields. Many DMEFTs already exist in the literature.[1] Various subsets of operators containing DM fields appear in refs. [14–25]. DM interactions with gluons and quarks as well as their impact on collider searches and direct detection for fermion and/or scalar DM particles are considered in refs. [26–28]. DM fermions coupling to photons are studied in refs. [29–31]. The authors of ref. [32] present a DMEFT containing scalars and fermions interacting with quarks, gluons and photons, and study the interactions at low energy scales. Loop effects from fermion DM particles are described in ref. [33], and matching conditions for the DMEFT at the EW scale are given in ref. [34]. Furthermore, in the context of co-annihilation, effective DM operators are discussed in refs. [35, 36].

---

[1]A discussion of non-relativistic DMEFTs can be found in refs. [1–13], for example.

Several more general analyses of full DMEFTs including higher dimensional operators exist. In ref. [37], an extension of the SM containing a scalar field in various representations is described. In ref. [38], the SM is extended by a Majorana fermion and a real scalar field, including operators up to dimension eight. A complete basis of operators including the SM fields together with a Majorana fermion is given in refs. [39–41], with an analysis of the impact of the operators on astroparticle and collider searches. In the context of hidden sector searches at colliders the authors of ref. [42] extend the SMEFT to include all portal operators up to dimension 5 withspin 0, 1/2 and 1 particles, while the extension of the LEFT includes all portal oper-ators up to dimension seven. A DMEFT which couples scalar, Dirac and vector DM particles to quarks and gluons is presented in ref. [42]. In ref. [43], a non-redundant set of operators including DM fields of spin ≤ 1 is considered. A discrete $\mathbb{Z}_2$ symmetry under which the DM particles are odd, whereas SM particles are even, is imposed so that the DM particles are stable. In ref. [44], a general EFT containing Dirac and Majorana fermions as well as complex and real scalar fields up to dimension-seven operators is presented, where the operators are assumed to be invariant under a global U(1) symmetry. In a recent work, the authors of ref. [45] discussed an extension of the SM Effective Field Theory (SMEFT) [46] with spin 0, 1/2 and 1 particles, presenting a general non-redundant basis of gauge-invariant operators up to dimension six. The DM fields are assumed to transform as electroweak multiplets with arbitrary weak isospin and hypercharge, and to respect a $\mathbb{Z}_2$ symmetry under which DM particles are odd.

A fully general DMEFT including scalar, fermion and vector DM fields in addition to the SM degrees of freedom, valid above and below the EW scale, is still missing, however. In this work, we close this gap by extending the SMEFT as well as the Low Energy Effective Field Theory (LEFT) [47, 48] by spin 0, 1/2 and 1 DM particles which are singlets under the SM gauge group. We construct the full set of non-redundant operators involving DM and SM fields up to dimension six, without imposing any underlying symmetry on the DM fields. The purely SM interactions above the EW scale are given by SMEFT [46], and below the EW scale by LEFT [47, 48], and we do not reproduce these operators here. The operators involving both SM and DM fields above the EW scale form a new EFT, called Dark SMEFT (DSMEFT), which is applicable for DM particles with masses above or below the EW scale, provided the new operators involving DM fields are invariant under the Standard Model $SU(3) \times SU(2) \times U(1)$ gauge symmetry and electroweak symmetry breaking is implemented via the usual Higgs mechanism.

A second EFT involving both SM and DM fields, called Dark LEFT (DLEFT), is a generalization of the LEFT to include spin 0, 1/2 and 1 DM singlet particles. DLEFT is applicable for light DM particles with masses below the EW scale interacting with light SM particles at energies below the EW scale, and does not make any assumptions about $SU(3) \times SU(2) \times U(1)$ invariance. The DLEFT operators are invariant under $SU(3) \times U(1)_{em}$ gauge symmetry. Like the LEFT, DLEFT does not contain the Higgs boson, and it can be considered without reference to DSMEFT for the light DM and light SM particles interacting at energies below the EW scale. DLEFT does not assume the Higgs mechanism for $SU(2) \times U(1)$ symmetry breaking.

Operators involving only DM fields are common to both DSMEFT and DLEFT, since only DM singlets are considered. For theories of light dark matter which use the SM Higgs

doublet to spontaneously break electroweak $SU(2) \times \text{U}(1)$ gauge symmetry, both DSMEFT and DLEFT apply, and we compute the tree-level matching conditions at the EW scale between the two theories when the heavy SM particles (t, h, Z, W) are integrated out, assuming that all dark matter particles are light and not integrated out at the EW scale. The results are easily generalized to the case where some dark matter particles are heavy by dropping operators containing those particles in DLEFT.

In addition to the general operator analysis, we also consider a specific DM matter scenario with vector dark matter which interacts with the SM via dimension-six operators involving three field-strength tensors, $F_\mu{}^\nu X_{a\nu}{}^\alpha X_{b\alpha}{}^\mu$ and $\widetilde{F}_\mu{}^\nu X_{a\nu}{}^\alpha X_{b\alpha}{}^\mu$. These are the only interactions of a light dark matter vector particle (i.e. in DLEFT) with the SM with dimension ≤ 6, if there is a $\mathbb{Z}_2$ symmetry in the dark sector. We work out the allowed parameter space of this model, and briefly discuss some of the phenomenological implications.

The paper is organized as follows. In section 2, we describe the assumptions made to construct the DSMEFT and the DLEFT. Section 3 analyzes a model containing two different vector DM particles, interacting with the SM photon through a dimension-six triple-gauge-field-strength interaction. We study the freeze-out and freeze-in scenarios, and plot the allowed region of parameter space. Conclusions are presented in section 4. The operator lists resulting from our general analysis are collected in the appendices. Appendix A presents the purely DM operators containing only DM fields up to dimension six. The purely DM operators in appendix A are common to both DSMEFT and DLEFT. Appendix B gives the DSMEFT operators involving both SM and DM fields up to dimension-six operators. Appendix C provides the DLEFT operators involving both SM and DM fields up to dimension-six operators. In all cases, the number of operators is given for n_ϕ dark scalars, n_χ dark fermions, n_X dark gauge bosons, and n_g SM generations. We also give the tree-level matching conditions between DSMEFT and DLEFT at the electroweak scale.

2 Dark matter EFT

In this section, we describe two new DMEFTs based on the SMEFT and the LEFT, which we call DSMEFT and DLEFT. The DM fields added to the field content of the effective theories are several copies of the spin 0, 1/2 and 1 fields ϕ, χ and X_μ, denoted by the generation index a. The DM fields are assumed to be singlets under the SM gauge group, and in particular to be electrically neutral. The scalar fields ϕ_a are real scalar fields, since a complex scalar field can be written in terms of two real scalar fields. The fermion fields χ_a are right-handed. We use right-handed DM fermions in order to make our results easier to compare with the extensive literature on right-handed sterile neutrinos. It is possible to write the same operators in terms of left-handed fermion fields which are the charge-conjugates of the right-handed fermion fields. Majorana fermions can be written in terms of right-handed Weyl fermions. The DM field content used in our analysis is summarized in table 1.

DM fields	ϕ	χ	X_μ
Spin	0	1/2	1
Number	n_ϕ	n_χ	n_X

Table 1. DM fields: ϕ is a real scalar field, χ is a *right-handed* fermion, and X_μ is a vector field. The DM fields are assumed to be singlets under the SM gauge group, so all DM fields are electrically neutral.

All DM particles are assumed to be light, with masses smaller than the EW scale, so the DM particles are present in the DMEFTs above as well as below the EW scale. When light ϕ, χ and X_μ fields are added to the SM field content, the most general gauge-invariant Lagrangian up to dimension six operators respecting the Standard Model $SU(3) \times SU(2) \times$ U(1) gauge symmetry defines DSMEFT, which generalizes the SMEFT theory to include light DM gauge particles which are gauge singlets. When light ϕ, χ and X_μ fields are added to the light SM fields contained in the LEFT, the most general gauge-invariant Lagrangian up to dimension six operators respecting the LEFT gauge symmetry $SU(3) \times$U(1)$_{\text{em}}$ defines DLEFT. Both DSMEFT and DLEFT contain purely DM operators, operators constructed only using DM fields. Since all DM particles are gauge singlets, the purely DM operators are identical for DSMEFT and DLEFT.

In order to keep the DSMEFT and DLEFT completely general, we do not impose any stabilizing symmetry on the DM fields. For specific applications, it is always possible to impose symmetries upon the general set of operators, reducing the operator set to a subset allowed by the symmetries. Consequently, the results of our operator analysis also apply outside the context of DM, namely for extensions of the SMEFT or LEFT with additional light degrees of freedom which are singlets under the SM gauge interactions.

The complete list of gauge-invariant operators up to mass dimension six built from DM and SM fields are collected in the appendices. For operators which are not hermitian, we have used +h.c. to denote that there are also hermitian conjugate operators which must be included, and which have the complex conjugate coefficient in the Lagrangian. Hermitian operators have a real coefficient in the Lagrangian. The purely DM operators are denoted by $\mathcal{P}$. The operators in DSMEFT are denoted by $\mathcal{Q}$ and those in DLEFT by $\mathcal{O}$, which are the same symbols used for the operators in SMEFT and LEFT, respectively. If the low-energy dark matter theory DLEFT arises as the low-energy limit of DSMEFT, we can compute the matching between the two dark matter theories. Operator coefficients in DLEFT get an additional matching contribution at the electroweak scale after integrating out the SM top quark, the Higgs boson and the W and Z gauge bosons. This additional matching piece is shown in the tables in appendices A and C.

The DM sector can have internal or gauge symmetries, which constrains the allowed coefficients. For example, if the n_ϕ scalars transform as the fundamental of a $SO(n_\phi)$ symmetry, the $\mathcal{P}_{\phi^3}$ operator is forbidden, and the $\mathcal{P}_{\phi^4}$ operator must be of the form $(\phi_a \phi_a)^2$. If the symmetry is gauged, so that DM particles couple to the X gauge bosons, then ordinary derivatives are replaced by covariant derivatives in the listed operators.

Appendix A contains the full set of purely DM operators, which are identical for DSMEFT and DLEFT. Appendix B gives the DSMEFT operators involving both SM and DM fields up to dimension-six operators. Appendix C provides the full set of DLEFT operators constructed from DM fields and the light SM fields with masses below the electroweak symmetry breaking scale up to dimension-six operators. In all of the three different operator sets we introduce an arbitrary number of DM particles of each type and count the number of independent operators. We have checked our results using the Python package `BasisGen` [49].

In the DM sector, we have included several operators $\mathcal{P}_\phi$, $\mathcal{P}_{\phi^2}$, $\mathcal{P}_\chi$, $\mathcal{P}_\phi^{\rm kin}$, $\mathcal{P}_\chi^{\rm kin}$, $\mathcal{P}_X^{\rm kin}$ which are usually not considered part of the EFT Lagrangian. The linear term $\mathcal{P}_\phi$ can be eliminated by shifting the ϕ field. The kinetic terms are usually brought to canonical form proportional to the unit matrix, and the mass terms are usually diagonalized. We have included these operators since there are matching contributions which shift their coefficients, so that even if the operators are put in standard form in DSMEFT, they are no longer in standard form in DLEFT. We would then have to make field transformations to put these operators back in standard form, which affects the matching to all the other operators, resulting in more complicated expressions.

The LEFT is constructed from the SMEFT by integrating out the heavy SM particles (t, h, Z and W) with an EW scale mass, leaving only the light SM particles. The Yukawa couplings of the light fermions are m_f/v. For consistency in the EFT power counting, these couplings should formally be treated as order $1/v$, i.e. the light fermion Yukawa interactions act formally like dimension-five operators rather than dimension-four operators. This power counting was used in refs. [47, 48] in computing the matching conditions between SMEFT and LEFT. The same analysis applies to the matching conditions between DSMEFT and DLEFT. A DM–SM interaction such as $H^\dagger H \phi^2$ gives a mass to the ϕ of order v^2 after EW symmetry breaking. Since our ϕ field is, *by assumption*, much lighter than the EW scale for it to be included in the DLEFT, the $H^\dagger H \phi^2$ operator has a coefficient suppressed by m_ϕ^2/v^2, and so the operator is effectively dimension six rather than dimension four. Other suppressed operators are given in appendix C.

3 A dark sector with two vectors

Dark abelian gauge bosons, also known as dark photons, are well studied [50]. They can interact with the SM through the renormalizable kinetic mixing portal (the DSMEFT operator $\mathcal{Q}_{BX}$ in table 9)

$$\mathcal{L}_{\rm mix} = \epsilon_a B_{\mu\nu} X_a^{\mu\nu} \ . \tag{3.1}$$

The interaction eq. (3.1) generates mixing between the dark photons X_a, and the U(1)$_Y$ SM gauge boson, which is a linear combination of the SM photon and Z boson. It consequently leads to decays of the dark photons into pairs of SM particles, e.g. $X_a \to e^+ e^-$. For the theory to be viable, the coupling ϵ_a must be tuned to be much smaller than unity, with typical values $\epsilon_a \sim 10^{-10}$.

In the following, we will consider a different scenario in which the dark sector consists of two dark vector particles, but the kinetic mixing portal operators eq. (3.1) are not present.[2] The absence of kinetic mixing with the SM U(1)$_Y$ gauge boson can be ensured by imposing a dark parity symmetry under which the dark vectors are odd $X_a^\mu \to -X_a^\mu$ but all SM particles are even. In such a case, the lightest dark vector is absolutely stable and the only relevant interactions between the dark vectors and SM particles up to dimension six are the dimension-six DSMEFT operators $\mathcal{Q}_{BX^2} = B_\mu{}^\nu X_{a\,\nu}{}^\alpha X_{b\,\alpha}{}^\mu$ and $\mathcal{Q}_{\widetilde{B}X^2} = \widetilde{B}_\mu{}^\nu X_{a\,\nu}{}^\alpha X_{b\,\alpha}{}^\mu$ from table 11.[3] $\mathcal{Q}_{BX^2}$ and $\mathcal{Q}_{\widetilde{B}X^2}$ are antisymmetric in the flavor indices a, b, so we need a minimum of two dark vectors for the interaction to exist.

Allowing for dark vector mass terms, we thus consider the Lagrangian

$$\begin{aligned}
\mathcal{L} = \mathcal{L}_{\mathrm{SM}} &- \frac{1}{4}X_1^{\mu\nu}X_{1\,\mu\nu} + \frac{m_1^2}{2}X_1^\mu X_{1\,\mu} - \frac{1}{4}X_2^{\mu\nu}X_{2\,\mu\nu} + \frac{m_2^2}{2}X_2^\mu X_{2\,\mu} \\
&+ C_{BX^2}B_\mu{}^\nu X_{1\,\nu}{}^\alpha X_{2\,\alpha}{}^\mu + C_{\widetilde{B}X^2}\widetilde{B}_\mu{}^\nu X_{1\,\nu}{}^\alpha X_{2\,\alpha}{}^\mu ,
\end{aligned} \tag{3.2}$$

where the SM U(1)$_Y$ gauge field B_μ is the linear combination $B_\mu = \cos\theta_W A_\mu - \sin\theta_W Z_\mu$ of the SM photon and the Z boson. The two couplings C_{BX^2} and $C_{\widetilde{B}X^2}$ have mass dimension -2. The dual field strength is $\widetilde{B}_{\mu\nu} = \frac{1}{2}\epsilon_{\mu\nu\alpha\beta}B^{\alpha\beta}$, where we use the sign convention $\epsilon_{0123} = +1$. The triple field-strength operator only exists if the three fields are *different*, so the interactions must involve two different DM gauge fields X_1 and X_2.

The vector boson mass terms arise from spontaneous symmetry breaking in the dark sector, e.g. by DM scalars. However, in this work, we do not consider the origin of the DM vector boson masses in detail, and merely assume the mass terms given in the above Lagrangian. A minimal mass generation mechanism is to have a U(1) gauge theory with a complex DM scalar for each X_μ boson. On spontaneous symmetry breaking, the angular component of the scalar gets eaten to give X_μ a mass, leaving behind the radial degree of freedom. The additional radial mode does not qualitatively affect the discussion of the model. It is easy to construct scenarios where its coupling to the SM is suppressed by Yukawa couplings or loop factors, and it makes small changes to the expansion rate and relic density of the universe. If the scalar mass is greater than twice the X_μ mass, any DM scalars produced in the early universe will decay into X_μ bosons. The scalar and gauge boson masses are independent, since they are proportional to the square-root of the ϕ^4 coupling, and the gauge coupling, respectively.

Λ is the new physics scale where one expects new degrees of freedom that interact with both the SM and the dark sector. Interactions with these new degrees of freedom can generate the dimension-six interactions in eq. (3.2) with C_{BX^2} and $C_{\widetilde{B}X^2}$ proportional to $1/\Lambda^2$. If the new physics is weakly coupled, the dimension-six operators are generated

---

[2]A similar model but expressed in terms of vector fields instead of field strength tensors has for instance been studied in [51, 52].

[3]DSMEFT can also have the dimension-six operators $\mathcal{Q}_{HX} = (H^\dagger H)X_{a\,\mu\nu}X_b^{\mu\nu}$ and $\mathcal{Q}_{H\widetilde{X}} = (H^\dagger H)\widetilde{X}_{a\,\mu\nu}X_b^{\mu\nu}$ which respect the dark matter $\mathbb{Z}_2$ symmetry. We neglect these operators — they do not lead to interactions with SM particles lighter than the electroweak scale at dimension six, as the Higgs coupling to SM particles is m/v, and is formally $1/\Lambda$ suppressed in the power counting for light particles. Their coefficients C_{BX^2} and $C_{\widetilde{B}X^2}$ do not enter the matching conditions to DLEFT up to dimension six.

at one-loop and have a $1/(16\pi^2)$ suppression. However strongly-interacting new physics theories need not have this suppression [53]. In our plots, we use $C_{BX^2} = 1/\Lambda^2$ as the definition of the new physics scale Λ. Without loss of generality we assume that X_1 is the lighter of the two dark vectors, $m_1 < m_2$, and therefore an absolutely stable dark matter candidate.

The vector X_2 is not stable; it can decay into X_1 and a photon, and, if kinematically allowed, into X_1 and a Z boson. Three-body decays mediated by a virtual photon or Z boson are necessarily suppressed compared to the two-body decay $X_2 \to X_1\gamma$, and are neglected in the following. For the decay rates $X_2 \to X_1\gamma$ and $X_2 \to X_1Z$ we find

$$\Gamma(X_2 \to X_1\gamma) = \frac{\cos^2\theta_W}{96\pi}(C_{BX^2}^2 + C_{\widetilde{B}X^2}^2)m_2^5(1+\varrho)(1-\varrho)^3 \,, \tag{3.3}$$

$$\begin{aligned}
\Gamma(X_2 \to X_1Z) = \frac{\sin^2\theta_W}{96\pi}m_2^5\,\lambda^{\frac{1}{2}}(1,\varrho,z)\Big[&C_{BX^2}^2(1+\varrho+z)\lambda(1,\varrho,z) \\
&+ C_{\widetilde{B}X^2}^2(1-(\varrho+z)-(\varrho^2+z^2)+(\varrho^3+z^3)+(6-\varrho-z)\varrho z)\Big],
\end{aligned} \tag{3.4}$$

where $\varrho = m_1^2/m_2^2$ is the ratio of squared dark vector masses, $z = m_Z^2/m_2^2$, and

$$\lambda(a,b,c) \equiv a^2 + b^2 + c^2 - 2(ab + ac + bc)\,. \tag{3.5}$$

We are mainly interested in the regime where the $X_2 \to X_1 + Z$ decay is kinematically forbidden.

If X_2 is produced in the early Universe, there are two viable regimes of X_2 lifetime τ_{X_2}, where $\tau_{X_2}^{-1} = \Gamma(X_2 \to X_1\gamma) + \Gamma(X_2 \to X_1Z)$. Either X_2 decays sufficiently quickly so that its decay does not significantly disrupt the element abundances predicted by big bang nucleosynthesis (BBN), or X_2 has an extremely long lifetime such that it can be effectively treated as stable, and the observed dark matter abundance has both a X_1 and a X_2 component. For a quickly decaying X_2, the BBN constraints are typically in the range $\tau_{X_2} \lesssim 1\,\mathrm{s}$ to $\tau_{X_2} \lesssim 10^4\,\mathrm{s}$, depending on the type and the energy spectrum of the visible decay products of X_2 [54–57]. We will use the conservative limit $\tau_{X_2} \lesssim 1\,\mathrm{s}$. A late-decaying X_2 component of dark matter can lead to distortions of the cosmic microwave background (CMB). If X_2 constitutes a significant fraction of the dark matter, its lifetime needs to be larger than approximately $\tau_{X_2} \gtrsim 10^{26}\,\mathrm{s}$ [57–60]. The two constraints combine to exclude the region $1\,\mathrm{s} \leq \tau_{X_2} \leq 10^{26}\,\mathrm{s}$.

If both X_1 and X_2 are sufficiently light, there is an additional contribution to the invisible Z width

$$\begin{aligned}
\Gamma(Z \to X_1X_2) = \frac{\sin^2\theta_W}{96\pi}m_Z^5\lambda^{\frac{1}{2}}(1,x_1,x_2)\Big[&C_{BX^2}^2(1+x_1+x_2)\lambda(1,x_1,x_2) \\
&+ C_{\widetilde{B}X^2}^2(1-(x_1+x_2)-(x_1^2+x_2^2)+(x_1^3+x_2^3)+(6-x_1-x_2)x_1x_2)\Big],
\end{aligned} \tag{3.6}$$

with $x_1 = m_1^2/m_Z^2$ and $x_2 = m_2^2/m_Z^2$. LEP measurements of the invisible width of the Z boson imply $\Gamma(Z \to X_1X_2) < 2.0\,\mathrm{MeV}$ at 95% C.L. [61].
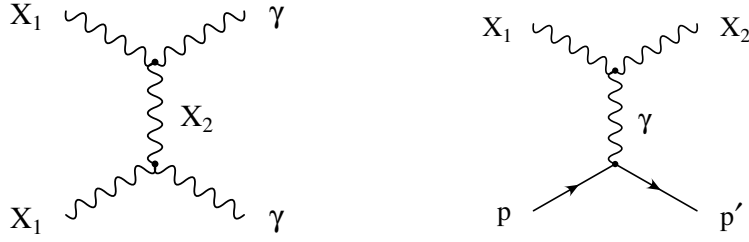
Figure 1. Left: example *t*-channel diagram for dark matter annihilation into photons. There is also the crossed *u*-channel diagram. Right: diagram for dark matter scattering off nuclei.

3.1 Dark matter production

Having defined the model, we consider in the following two possibilities for dark matter production: freeze-out and freeze-in. In both cases we discuss which values of the new physics parameters (the masses m_1 and m_2 and new physics scale Λ) can give the observed dark matter abundance $\Omega h^2 \simeq 0.12$ [62].

3.1.1 Freeze-out

If the interactions between the SM sector and the dark sector are large enough that the two sectors are in thermal equilibrium in the early universe, the dark matter abundance is set by freeze-out as the universe cools. The correct dark matter relic abundance can be obtained if the annihilation cross section of dark matter into SM particles is of electroweak size. To a good approximation one finds

$$\Omega h^2 \simeq 0.12 \times \left(\frac{2.2 \times 10^{-26} \text{cm}^3/\text{s}}{\langle \sigma v_{\text{rel}} \rangle} \right) , \tag{3.7}$$

where $\langle \sigma v_{\text{rel}} \rangle$ is the thermal average of the dark matter annihilation cross section times the relative dark matter velocity.

Dark matter annihilation can occur through several channels, in particular $X_1 X_1 \to \gamma\gamma$, $X_1 X_1 \to Z\gamma$, and $X_1 X_1 \to ZZ$ through *t*-channel or *u*-channel X_2 exchange, see the left diagram in figure 1. Co-annihilation channels like $X_1 X_2 \to WW$, $X_1 X_2 \to Zh$, or $X_1 X_2 \to \bar{f}f$ through an *s*-channel photon or Z boson, where f is a SM fermion, can be relevant for $m_1 \simeq m_2$, so that there is an appreciable density of X_2. For the $X_1 X_1 \to \gamma\gamma$ annihilation cross section, we find

$$\sigma(X_1 X_1 \to \gamma\gamma)v_{\text{rel}} = \cos^4 \theta_W \left(C_{BX^2}^2 + C_{\tilde{B}X^2}^2 \right)^2 \frac{m_1^6}{144\pi} \left\{ \frac{5\varrho^2}{(1+\varrho)^2} \right.$$
$$\left. + v_{\text{rel}}^2 \frac{\varrho^2(167 + 194\varrho + 71\varrho^2)}{12(1+\varrho)^4} \right\} + O(v_{\text{rel}}^4) , \tag{3.8}$$

where as above, $\varrho = m_1^2/m_2^2$, and we have expanded to second order in the relative velocity. An analogous expression holds for the cross section $\sigma(X_2 X_2 \to \gamma\gamma)v_{\text{rel}}$, with $m_1 \leftrightarrow m_2$.

The thermal averages of powers of the relative velocity scale as $\langle v_{\text{rel}}^{2n} \rangle \sim x^{-n}$, where $x^{-1} = T_{\text{fo}}/m$ with m the dark matter mass and T_{fo} the temperature at freeze-out. Typically,

$T_{\text{fo}}/m \sim 1/20$. Therefore, it is a good approximation to keep only the leading term in the v_{rel} expansion. Based on the $X_1 X_1 \to \gamma\gamma$ annihilation channel alone, we find

$$\langle \sigma v_{\text{rel}} \rangle = \frac{5 \cos^4 \theta_W}{144\pi} \left(C_{BX^2}^2 + C_{\widetilde{B}X^2}^2 \right)^2 m_1^6 \frac{\varrho^2}{(1+\varrho)^2} + \mathcal{O}(T_{\text{fo}}/m) \,. \tag{3.9}$$

Using the approximate expression for the relic abundance from above, and demanding that X_1 gives all of the dark matter, we find a new physics scale of

$$\Lambda \sim \left(C_{BX^2}^2 + C_{\widetilde{B}X^2}^2 \right)^{-\frac{1}{4}} \sim 104 \,\text{GeV} \times \left(\frac{m_1}{50 \,\text{GeV}} \right)^{\frac{3}{4}} \left[\frac{4\varrho^2}{(1+\varrho)^2} \right]^{\frac{1}{8}} \,. \tag{3.10}$$

This scale is close to the electroweak scale for $m_1 \sim 50 \,\text{GeV}$, and gets even smaller for lighter X_1. Including the other annihilation channels will modify this estimate for Λ by an amount of order one. Such a low new physics scale is challenged by the absence of direct evidence for new degrees of freedom at the LHC and we therefore will not pursue the freeze-out scenario in more detail.

3.1.2 Freeze-in

In the freeze-in scenario, the interactions between the SM and the dark sector are so feeble that the two sectors do not reach thermal equilibrium. We assume that after reheating there is a negligible abundance of dark matter, and dark matter particles get produced from decays or scattering of SM particles [63]. In our setup, higher dimensional operators parameterize the interactions between the dark matter sector and the SM, similar to the scenarios discussed in ref. [64]. For a sufficiently large new physics scale Λ, the interactions are feeble enough to realize the dark matter freeze-in scenario. The formulation in terms of higher dimensional operators is consistent as long as the reheat temperature T_{rh} is much smaller than the new physics scale Λ.

We briefly review the freeze-in formalism, following largely ref. [65]. The number densities n_{X_1} and n_{X_2} of the dark sector particles X_1 and X_2 are determined by the Boltzmann equations

$$\begin{aligned}
\dot{n}_{X_1} + 3Hn_{X_1} &= C_{\gamma\gamma \to X_1 X_1} + C_{Z\gamma \to X_1 X_1} + C_{ZZ \to X_1 X_1} \\
&\quad + C_{Zh \to X_1 X_2} + C_{WW \to X_1 X_2} + \sum_f C_{\bar{f}f \to X_1 X_2} \,,
\end{aligned} \tag{3.11}$$

$$\begin{aligned}
\dot{n}_{X_2} + 3Hn_{X_2} &= C_{\gamma\gamma \to X_2 X_2} + C_{Z\gamma \to X_2 X_2} + C_{ZZ \to X_2 X_2} \\
&\quad + C_{Zh \to X_1 X_2} + C_{WW \to X_1 X_2} + \sum_f C_{\bar{f}f \to X_1 X_2} \,,
\end{aligned} \tag{3.12}$$

where H is the Hubble parameter, and the collision terms on the right-hand side take into account dark matter production from the scattering processes $\gamma\gamma \to X_i X_i$, $Z\gamma \to X_i X_i$, and $ZZ \to X_i X_i$ that involve two dimension-six interactions, as well as the processes $Zh \to X_1 X_2$, $WW \to X_1 X_2$, and $\bar{f}f \to X_1 X_2$ that are mediated by an s-channel Z or γ and involve only a single dimension-six interaction. The collision terms are given explicitly in eqs. (3.20)–(3.25), and include the final state multiplicities. The $X_1 X_2$ processes, which

are order $1/\Lambda^4$, dominate over the $X_1 X_1$ and $X_2 X_2$ processes of order $1/\Lambda^8$ if $m_1 \sim m_2$. Otherwise, the relative rates depend also on the Boltzmann suppression for X_2.

It is convenient to rewrite the Boltzmann equations in terms of the comoving number densities $Y_{X_i} = n_{X_i}/\mathsf{s}$ where s is the entropy density. One finds

$$
\begin{aligned}
Y_{X_1} = \int_{T_0}^{T_{\rm rh}} \frac{dT}{T} \frac{1}{\mathsf{s}H} &(C_{\gamma\gamma \to X_1 X_1} + C_{Z\gamma \to X_1 X_1} + C_{ZZ \to X_1 X_1} \\
&+ C_{Zh \to X_1 X_2} + C_{WW \to X_1 X_2} + \sum_f C_{\bar{f}f \to X_1 X_2}),
\end{aligned}
\tag{3.13}
$$

$$
\begin{aligned}
Y_{X_2} = \int_{T_0}^{T_{\rm rh}} \frac{dT}{T} \frac{1}{\mathsf{s}H} &(C_{\gamma\gamma \to X_2 X_2} + C_{Z\gamma \to X_2 X_2} + C_{ZZ \to X_2 X_2} \\
&+ C_{Zh \to X_1 X_2} + C_{WW \to X_1 X_2} + \sum_f C_{\bar{f}f \to X_1 X_2}),
\end{aligned}
\tag{3.14}
$$

where $T_0 \simeq 0$ is the temperature today, and the entropy density and Hubble parameter are given by

$$
\mathsf{s} = \frac{2\pi^2}{45} g_\star T^3 , \qquad\qquad H = \frac{\pi}{3\sqrt{10}} \sqrt{g_\star} \frac{T^2}{M_{\rm Pl}} , \tag{3.15}
$$

with $M_{\rm Pl} \simeq 2.4 \times 10^{18}\,{\rm GeV}$ the reduced Planck mass, and $g_\star$ the effective number of degrees of freedom. In eqs. (3.13), (3.14), we have approximated the effective number of degrees of freedom in the thermal bath for the entropy and energy density as a constant, $g_\star^s = g_\star^\rho = g_\star = {\rm const}$. This is a good approximation for temperatures above the electroweak scale [66]. For such temperatures, $g_\star \simeq 427/4$ in the SM.

We identify two qualitatively different scenarios that are determined by the hierarchy of the scales m_1, m_2, and $T_{\rm rh}$:

(1) $m_1 < T_{\rm rh} < m_2$: in this case only X_1 can be produced by the scattering of SM particles. The s-channel production modes that include X_2 in the final state are kinematically suppressed. The dark matter abundance is therefore given by

$$
\Omega h^2 = \frac{h^2 \mathsf{s}_0}{\rho_{\rm crit}} m_1 Y_{X_1} \simeq (2.7 \times 10^8) \left(\frac{m_1}{1\,{\rm GeV}} \right) Y_{X_1} , \tag{3.16}
$$

where $\rho_{\rm crit} = 1.053672(24) \times 10^{-5} h^2\,{\rm GeV/cm^3}$ [67] is the critical density of the Universe and $\mathsf{s}_0 = 2891.2(1.9)/{\rm cm^3}$ [67] is the entropy density today. If the reheat temperature $T_{\rm rh}$ is significantly below the electroweak scale, the only relevant process that produces dark matter, and that needs to be taken into account in the calculation of comoving number density Y_{X_1} is $\gamma\gamma \to X_1 X_1$. For $T_{\rm rh}$ above the electroweak scale, $Z\gamma \to X_1 X_1$ and $ZZ \to X_1 X_1$ also need to be considered.

(2) $m_1 < m_2 < T_{\rm rh}$: in this case, both X_1 and X_2 are produced by the scattering of SM particles. To obtain the dark matter abundance we need to distinguish two sub-cases:

(2a) the lifetime of X_2 is much larger than the age of the universe. In this case dark matter is made from two components, the absolutely stable X_1 and the

approximately stable X_2 and the corresponding abundances add up

$$\Omega h^2 = \frac{h^2 \mathsf{s}_0}{\rho_{\text{crit}}}(m_1 Y_{X_1} + m_2 Y_{X_2}) \simeq (2.7 \times 10^8) \left[\left(\frac{m_1}{1\,\text{GeV}}\right) Y_{X_1} + \left(\frac{m_2}{1\,\text{GeV}}\right) Y_{X_2}\right].$$
(3.17)

(2b) the lifetime of X_2 is much shorter than the age of the universe. In this case, X_2 has decayed through the processes $X_2 \to X_1 \gamma$ and, if kinematically allowed, $X_2 \to X_1 Z$, producing one X_1 particle per decaying X_2 particle. The relic density therefore is

$$\Omega h^2 = \frac{h^2 \mathsf{s}_0}{\rho_{\text{crit}}} m_1 (Y_{X_1} + Y_{X_2}) \simeq (2.7 \times 10^8) \left(\frac{m_1}{1\,\text{GeV}}\right)(Y_{X_1} + Y_{X_2}).$$
(3.18)

For a reheat temperature below the electroweak scale, only processes with photons and light SM fermions need to be taken into account when calculating Y_{X_1} and Y_{X_2}. For sufficiently large T_{rh}, all processes in (3.13) and (3.14) are relevant.

To evaluate the relic density, we need to determine the various collision terms. In the case of $2 \to 2$ scattering one has the following generic expression

$$C_{ab \to cd} \simeq \int \frac{d^3 p_a}{(2\pi)^3 2E_a} \int \frac{d^3 p_b}{(2\pi)^3 2E_b} \int \frac{d^3 p_c}{(2\pi)^3 2E_c} \int \frac{d^3 p_d}{(2\pi)^3 2E_d}$$
$$\times f_a^{\text{eq}}(E_a) f_b^{\text{eq}}(E_b)|\overline{\mathcal{M}}_{ab \to cd}|^2 (2\pi)^4 \delta^{(4)}(p_a + p_b - p_c - p_d),$$
(3.19)

since the final state occupation numbers $f_c^{\text{eq}}(E_c)$, $f_d^{\text{eq}}(E_d) \ll 1$ so we can neglect final state Bose and Fermi factors. Note that the squared matrix elements are summed over both initial and final state degrees of freedom (e.g. spins, polarizations, color). The equilibrium phase space distributions are to a good approximation given by $f_i^{\text{eq}}(E_i) \simeq \exp(-E_i/T)$. Carrying out the momentum integrations, the collision terms for the scattering processes can be related to the corresponding scattering cross sections. We find (including the multiplicity of the final state in the definition of the collision integral)

$$C_{\gamma\gamma \to X_i X_i} = \frac{1}{8\pi^4} T \int_0^\infty ds\ s^{\frac{3}{2}} K_1(\sqrt{s}/T) \sigma(\gamma\gamma \to X_i X_i),$$
(3.20)

$$C_{ZZ \to X_i X_i} = \frac{9}{32\pi^4} T \int_{4m_Z^2}^\infty ds\ s^{\frac{3}{2}} K_1(\sqrt{s}/T) \left(1 - \frac{4m_Z^2}{s}\right) \sigma(ZZ \to X_i X_i),$$
(3.21)

$$C_{Z\gamma \to X_i X_i} = \frac{3}{8\pi^4} T \int_{m_Z^2}^\infty ds\ s^{\frac{3}{2}} K_1(\sqrt{s}/T) \left(1 - \frac{m_Z^2}{s}\right)^2 \sigma(Z\gamma \to X_i X_i),$$
(3.22)

$$C_{WW \to X_1 X_2} = \frac{9}{32\pi^4} T \int_{4m_W^2}^\infty ds\ s^{\frac{3}{2}} K_1(\sqrt{s}/T) \left(1 - \frac{4m_W^2}{s}\right) \sigma(WW \to X_1 X_2),$$
(3.23)

$$C_{Zh \to X_1 X_2} = \frac{3}{32\pi^4} T \int_{(m_Z+m_h)^2}^\infty ds\ s^{\frac{3}{2}} K_1(\sqrt{s}/T) \lambda\left(1, \frac{m_Z^2}{s}, \frac{m_h^2}{s}\right) \sigma(Zh \to X_1 X_2),$$
(3.24)

$$C_{\bar{f}f \to X_1 X_2} = \frac{N_c^2}{8\pi^4} T \int_{4m_f^2}^\infty ds\ s^{\frac{3}{2}} K_1(\sqrt{s}/T) \left(1 - \frac{4m_f^2}{s}\right) \sigma(\bar{f}f \to X_1 X_2),$$
(3.25)

with a color factor $N_c = 3$ for quarks and $N_c = 1$ for leptons. $\lambda(a, b, c)$ is defined in eq. (3.5), and K_1 is the first modified Bessel function of the second kind.

In the following we will focus on two benchmark cases that are representative for the generic scenarios (1) and (2) identified above. A comprehensive discussion of the entire parameter space is beyond the scope of this work.

For the first benchmark case we assume that the reheat temperature is below both the electroweak scale and the mass of the second vector X_2. Thus, only the $\gamma\gamma \to X_1 X_1$ collision term is relevant. Furthermore, if the mass of X_1 is sufficiently small, $m_1 \ll T_{\rm rh} \ll m_2$, we find the following simple expression for the cross section

$$\sigma(\gamma\gamma \to X_1 X_1) \simeq \frac{263\cos^4\theta_W}{215040\pi} \frac{s^5}{m_2^4}(C_{BX^2}^2 + C_{\widetilde{B}X^2}^2)^2\,, \tag{3.26}$$

where s is the diphoton invariant mass. Neglecting the temperature dependence of the effective number of degrees of freedom $g_\star$, the corresponding collision term and the resulting comoving X_1 number density can be determined analytically. We find

$$C_{\gamma\gamma \to X_1 X_1} \simeq \frac{9089280\cos^4\theta_W}{\pi^5} \frac{T^{16}}{m_2^4}(C_{BX^2}^2 + C_{\widetilde{B}X^2}^2)^2\,, \tag{3.27}$$

$$Y_{X_1} \simeq \frac{613526400\sqrt{10}}{11\pi^8} \frac{\cos^4\theta_W}{g_\star^{3/2}} \frac{M_{\rm pl}T_{\rm rh}^{11}}{m_2^4}(C_{BX^2}^2 + C_{\widetilde{B}X^2}^2)^2\,. \tag{3.28}$$

If the reheat temperature is above the electroweak scale, the comoving number density increases by an $\mathcal{O}(1)$ amount due to the additional $ZZ \to X_1 X_1$ and $\gamma Z \to X_1 X_1$ channels, but the characteristic dependence on $T_{\rm rh}^{11}$ does not change. The correct dark matter abundance, $\Omega h^2 \simeq 0.12$, is obtained for a new physics scale Λ approximately 3 orders of magnitude above the reheat temperature

$$\frac{\Lambda}{T_{\rm rh}} = \frac{(C_{BX^2}^2 + C_{\widetilde{B}X^2}^2)^{-\frac{1}{4}}}{T_{\rm rh}} \sim 700 \times \left(\frac{m_1}{1\,{\rm GeV}}\right)^{\frac{1}{8}} \times \left(\frac{T_{\rm rh}}{100\,{\rm GeV}}\right)^{\frac{3}{8}} \times \left(\frac{1\,{\rm TeV}}{m_2}\right)^{\frac{1}{2}} \times \left(\frac{100}{g_\star}\right)^{\frac{3}{16}}\,. \tag{3.29}$$

This is consistent with our assumption that the EFT description of the dark vector interactions is appropriate to determine the dark matter abundance.

In the second benchmark case we assume again that the reheat temperature is below the electroweak scale but this time both X_1 and X_2 are significantly lighter, $m_1, m_2 \ll T_{\rm rh}$. In this case, the dominant dark matter production process is $f\bar{f} \to X_1 X_2$ mediated by an s-channel photon. The corresponding amplitude is suppressed by only one power of the dimension-six dark vector interaction with the photon. For the cross section we find (assuming for simplicity also $m_f \ll T_{\rm rh}$)

$$\sigma(\bar{f}f \to X_1 X_2) \simeq \frac{Q_f^2 e^2 \cos^2\theta_W}{96\pi N_c}s(C_{BX^2}^2 + C_{\widetilde{B}X^2}^2)\,, \tag{3.30}$$

where Q_f is the electric charge of the fermion f. The corresponding collision term and the resulting comoving number densities are

$$C_{\bar{f}f \to X_1 X_2} \simeq N_c Q_f^2 \frac{e^2\cos^2\theta_W}{\pi^5}T^8(C_{BX^2}^2 + C_{\widetilde{B}X^2}^2)\,, \tag{3.31}$$
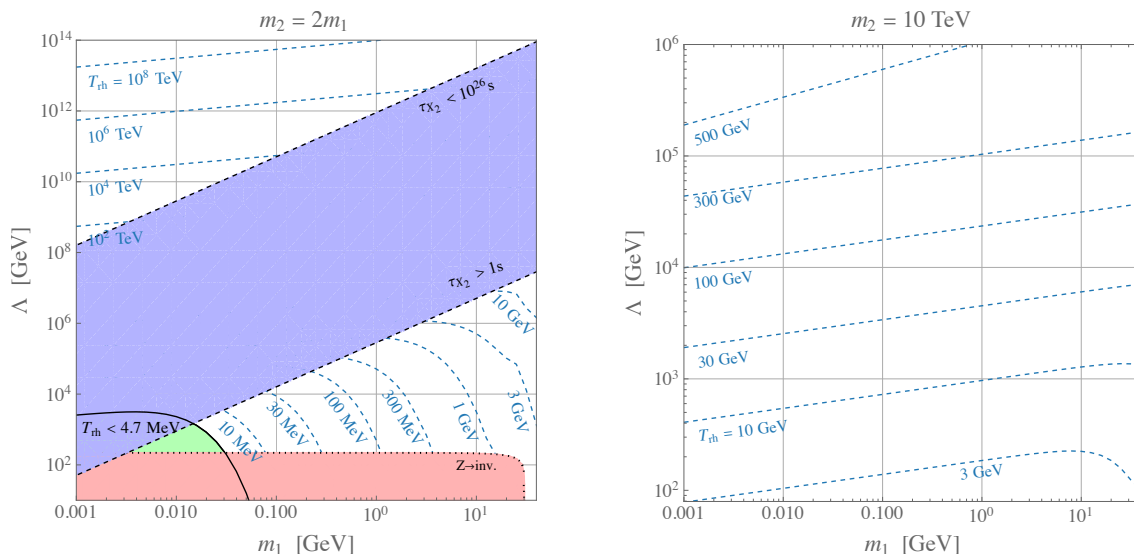
Figure 2. Reheat temperature to reproduce the observed dark matter abundance. The curves have been evaluated for $C_{\widetilde{B}X^2} = 0$ and $C_{BX^2} = 1/\Lambda^2$. The red shaded region is excluded by the invisible width of the Z, the blue shaded region by lifetime constraints on X_2, and the green shaded region by the limit $T_{\rm rh} < 4.7\,{\rm MeV}$ from the CMB and BBN [68].

$$Y_{X_1} \simeq Y_{X_2} \simeq \frac{45\sqrt{10}}{2\pi^8} \sum_f N_c Q_f^2 \, \frac{e^2 \cos^2\theta_W}{g_\star^{3/2}} M_{\rm pl} T_{\rm rh}^3 \big(C_{BX^2}^2 + C_{\widetilde{B}X^2}^2\big) \ . \tag{3.32}$$

For reheat temperatures above the electroweak scale, the comoving number densities will be larger by an $\mathcal{O}(1)$ amount, because additional dark matter production channels open up. The dominant channels all scale with $T_{\rm rh}^3$. Summing over all charged leptons and the five light quarks, $\sum_f N_c Q_f^2 = 20/3$. Assuming the vector X_2 decays sufficiently fast, we find the following new physics scale to reproduce the observed dark matter abundance

$$\frac{\Lambda}{T_{\rm rh}} = \frac{(C_{BX^2}^2 + C_{\widetilde{B}X^2}^2)^{-\frac{1}{4}}}{T_{\rm rh}} \sim \left(1.43 \times 10^5\right) \times \left(\frac{m_1}{1\,{\rm GeV}}\right)^{\frac{1}{4}} \times \left(\frac{100\,{\rm GeV}}{T_{\rm rh}}\right)^{\frac{1}{4}} \times \left(\frac{100}{g_\star}\right)^{\frac{3}{8}} \ . \tag{3.33}$$

In figure 2, we show the new physics scale Λ as a function of m_1, the mass of the dark matter particle, for different values of the reheat temperature $T_{\rm rh}$. In both plots, the new physics scale Λ is always considerably greater than $T_{\rm rh}$ so the EFT computation of the cross sections is valid. For simplicity, we only show the case where $C_{\widetilde{B}XX} = 0$. Including both the BXX and $\widetilde{B}XX$ operators makes only small differences in the plots. In the plots, we have included the full mass-dependence of the cross sections, rather than the simplified expressions in eqs. (3.26), (3.31). The $f\bar{f} \to X_1 X_2$ cross section used includes both γ and Z exchange, rather than just γ exchange given in eq. (3.31). We have also included all the collision integrals in the numerical calculations, as well as the temperature dependence of $g_\star$. The processes which produce $X_1 X_2$ in the final state have one insertion of the dimension-six interaction, so the cross section is proportional to $1/\Lambda^4$. Processes with $X_1 X_1$ or $X_2 X_2$ in the final state have two insertions of the dimension-six interaction, and are proportional to $1/\Lambda^8$.

The left-hand plot has two light vectors with $m_2 = 2m_1$. In this case the freeze-in is dominated by processes that produce $X_1 X_2$ from the scattering of two SM particles. We evaluated the collision integrals and the relic abundance numerically. For reheat temperatures much larger than m_1 and m_2, the analytic result in (3.33) is a very good approximation and the shown curves follow the relation $\Lambda \propto m_1^{1/4}$. For reheat temperatures of the order of m_1 or even smaller, the analytic result no longer holds and we observe a qualitatively different behavior of the curves. Note that for very small $T_{\rm rh} \lesssim \Lambda_{\rm QCD}$ one should not evaluate the collision terms based on quarks, but rather work with hadrons. However, we do not expect the qualitative behavior to change in this region of parameter space.

Certain regions of the plot are excluded. The X_2 lifetime should be greater than 10^{26} s to avoid distortions of the CMB, or less than 1 s to avoid affecting the elemental abundances predicted by BBN. We also show the disallowed region from the invisible decay width of the Z and from the limit on the reheat temperature $T_{\rm rh} < 4.7\,{\rm MeV}$ from the CMB and BBN [68].

The right-hand plot has one heavy vector with a mass $m_2 = 10\,{\rm TeV}$ and one light vector. In this case the dark matter freeze-in is largely determined by the process $\gamma\gamma \to X_1 X_1$ for low reheat temperatures. Other processes such as $ZZ \to X_1 X_1$ and $\gamma Z \to X_1 X_1$ are relevant if $T_{\rm rh}$ is sufficiently large, and are included in the numerics. The $\bar{f}f \to X_1 X_2$ processes become relevant in the upper part of the plot where $T_{\rm rh}$ is only slightly smaller than m_2. As for the left-hand plot, we evaluate the collision integrals and the relic abundance numerically. For most of the plot, the analytical expression (3.29) is a very good approximation and the curves follow $\Lambda \propto m_1^{1/8}$.

For completeness, we give the $WW \to X_1 X_2$ and $Zh \to X_1 X_2$ cross sections in the limit $m_1, m_2 \to 0$, where the expressions simplify considerably:

$$\sigma(W^+ W^- \to X_1 X_2) = \frac{e^2 c_W^2 (C_{BX^2}^2 + C_{\tilde{B}X^2}^2) M_Z^4 s^{1/2} \sqrt{s - 4M_W^2}}{3456\pi (s - M_Z^2)^2 M_W^4} (12M_W^4 + 20M_W^2 s + s^2),$$

(3.34)

$$\sigma(hZ \to X_1 X_2) = \frac{e^2 (C_{BX^2}^2 + C_{\tilde{B}X^2}^2) s^2}{1152\pi c_W^2 (s - M_Z^2)^2 \sqrt{s^2 - 2s(M_Z^2 + M_H^2) + (M_Z^2 - M_H^2)^2}} \times$$
$$\left[s^2 + 2s(5M_Z^2 - M_H^2) + (M_H^2 - M_Z^2)^2 \right].$$

(3.35)

In the numerics, we have used the complete expressions for the cross sections.

3.2 Dark matter signatures

Dark matter that is frozen-in is characterized by very feeble interactions with the SM. Models of dark matter freeze-in are therefore generically hard to probe. One expects tiny scattering cross sections of the local dark matter on SM targets, tiny annihilation rates of galactic dark matter to SM particles, and tiny rates of dark matter production at particle colliders. In the following we briefly discuss the scattering of the dark matter on SM fermions in the model presented above.
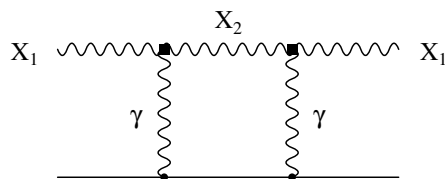
Figure 3. Graph contributing to the elastic scattering $X_1 + f \to X_1 + f$ off fermions such as electrons or nuclei in the target. The boxes are insertions of the dimension-six interaction.

Elastic scattering of the dark matter particle X_1 on nuclei or electrons can be mediated by a loop of X_2 and photons (or Z bosons) that involves two of the dimension 6 interactions, such as the graph shown in figure 3. The corresponding cross sections $\sigma(X_1N \to X_1N)$ and $\sigma(X_1e \to X_1e)$ are suppressed by a loop factor and eight powers of the new physics scale Λ. These direct detection cross sections are therefore exceedingly small in the regions of parameter space that give the right dark matter abundance.

If both dark vectors X_1 and X_2 are almost degenerate, $m_1 \simeq m_2$, one can have inelastic scattering at tree level as shown on the right hand side of figure 1. The corresponding cross section scales as $1/\Lambda^4$. As long as the inelastic processes $X_1N \to X_2N$ and $X_1e \to X_2e$ are kinematically allowed, they are parametrically much larger than the elastic scattering processes. We first consider the case where X_2 is short-lived, so that the dark matter is X_1. As the local dark matter has speeds of the order of $v \sim 10^{-3}$, the mass splitting between X_2 and X_1 should be at most $\Delta = m_2 - m_1 \sim 10^{-6}m_1$ for inelastic scattering to be kinematically allowed. For inelastic dark matter scattering on a fermion f we find the cross section near threshold

$$\sigma(f + X_1 \to f + X_2) = w \frac{e^2 Q_f^2 c_W^2 m_1^{1/2} m_2^{5/2}}{24\pi\sqrt{2}(m_2^2 - m_1^2)^{3/2}(m_f + m_2)^3 \sqrt{(2m_f + m_2)^2 - m_1^2}} \times$$

$$\left\{ C_{BX^2}^2 \left(m_2^2 - m_1^2 \right) \left[(2m_f + m_2)^2 - m_1^2 \right] \left(m_1^2 + m_2^2 + 4m_f^2 \right) \right.$$

$$+ C_{\tilde{B}X^2}^2 \left[(m_1^2 + m_2^2)(m_2^2 - m_1^2)^2 + 4m_f m_2(m_2^2 - m_1^2)^2 + 8m_f^2 \left(m_2^4 + m_1^4 \right) \right.$$

$$\left. \left. + 16m_f^3 m_2(m_1^2 + m_2^2) + 16m_f^4 m_2^2 \right] \right\} + \dots \tag{3.36}$$

Here

$$s = (m_f + m_2)^2 + 2m_f m_1 w^2, \qquad\qquad w \ll 1 \tag{3.37}$$

is the expansion of s near threshold in terms of a dimensionless parameter w. The relative boost γ between X_1 and f is

$$\gamma = \frac{p_1 \cdot k_1}{m_1 m_f} = \frac{m_2^2 - m_1^2 + 2m_f m_2 + 2m_f m_1 w^2}{2m_1 m_f} = \frac{m_2^2 - m_1^2 + 2m_f m_2}{2m_1 m_f} + w^2 \tag{3.38}$$

so w^2 is the deviation of γ from the minimum value required for X_2 production to be kinematically allowed. Since incident dark matter particles are non-relativistic, we can

further simplify the cross section by expanding in the mass difference $\Delta = m_2 - m_1$, giving

$$\sigma(f + X_1 \to f + X_2) = \frac{C_{\tilde{B}X^2}^2 e^2 Q_f^2 c_W^2 m_f^{3/2} m_1^{7/2} w}{12\pi \Delta^{3/2} (m_f + m_1)^{3/2}} + \dots \tag{3.39}$$

The t-channel infrared singularity in the total photon exchange cross section is regulated by the finite mass difference Δ.

For a non-relativistic X_1 with velocity v incident on a fermion at rest,

$$w^2 \approx \frac{4m_f m_1 v^2 + m_1^2 v^4 - 8(m_1 + m_f)\Delta - 4\Delta^2}{8m_f m_1}. \tag{3.40}$$

As an example, consider the case of X_1 with mass $m_1 = 1\,\text{GeV}$ incident with a typical dark matter velocity $v = 10^{-3}$ on a nucleon target with $m_f = 1\,\text{GeV}$. From eq. (3.40), $w^2 \approx 5 \times 10^{-7} - 2\Delta/(1\,\text{GeV})$, and X_2 production is kinematically allowed only if $\Delta \leq 0.25\,\text{keV}$. This shows that X_1 and X_2 have to be almost degenerate for the scattering process to be kinematically allowed for incident particles with typical dark matter velocities. For $\Delta \sim 0.1\,\text{keV}$, $\sigma(f + X_1 \to f + X_2) \approx 5 \times 10^{-24} \times (1\,\text{GeV}/\Lambda)^4\,\text{cm}^2$ leading to a collision rate $\Gamma \approx (1\,\text{GeV}/\Lambda)^4 \times 10^{-22}\,\text{s}^{-1}$ per target nucleon, assuming X_1 is all of the local dark matter density. The nuclear recoil energy is of order Δ, and is approximately $0.1\,\text{keV}$. These numbers show that direct detection of X_1 is not a realistic possibility — X_1 and X_2 have to be nearly degenerate, the nuclear recoil energy is low, and the collision rate is small for Λ much above the electroweak scale.

In some regions of parameter space (the upper part of the left-hand plot in figure 2), X_2 is long-lived, and the dark matter is equal parts X_1 and X_2. In this region, one can also have the exothermic reaction $f + X_2 \to f + X_1$. We expand the cross section near threshold in w where

$$s = (m_2 + m_f)^2 + 2m_f m_2 w^2, \qquad\qquad w \ll 1. \tag{3.41}$$

Here the relative boost of the incoming particles is

$$\gamma = \frac{p_2 \cdot k_1}{m_2 m_f} = 1 + w^2 \tag{3.42}$$

so that $w^2 \approx v^2/2$ for $v \ll 1$, where X_2 particles of velocity v are incident on fermions at rest. The expanded cross section is

$$\sigma(f + X_2 \to f + X_1) = \frac{1}{w} \frac{e^2 Q_f^2 c_W^2 m_2 \sqrt{(m_2 + 2m_f)^2 - m_1^2}}{192\pi\sqrt{2}m_f^2 \sqrt{m_2^2 - m_1^2}(m_f + m_2)^3} \times$$

$$\left\{ C_{BX^2}^2 \left[(m_2 + 2m_f)^2 - m_1^2 \right] \left[m_2^2 - m_1^2 \right] \left[m_1^2 + m_2^2 + 4m_f^2 \right] \right.$$

$$+ C_{\tilde{B}X^2}^2 \left[16m_f^4 m_2^2 + 16m_f^3 m_2(m_1^2 + m_2^2) \right.$$

$$\left. \left. + 8m_f^2(m_1^4 + m_2^4) + 4m_f m_2(m_2^2 - m_1^2)^2 + (m_2^2 - m_1^2)^2(m_1^2 + m_2^2) \right] \right\} + \dots \tag{3.43}$$

For the case of $m_1 = 1\,\text{GeV}$, $m_2 = 2\,\text{GeV}$ incident on a nucleon target $m_f = 1\,\text{GeV}$, $\sigma(f + X_2 \to f + X_1) \approx 3 \times 10^{-27} \times (1\,\text{GeV}/\Lambda)^4\,\text{cm}^2$ leading to a collision rate $\Gamma \approx (1\,\text{GeV}/\Lambda)^4 \times 2 \times 10^{-26}\,\text{s}^{-1}$ assuming that equal amounts of X_1 and X_2 form the local dark matter density. For $\Lambda \sim 10^{12}\,\text{GeV}$, typical values for Λ in this region of parameter space, the reaction rate is too small to be detected in laboratory experiments [69].

Another possible detection mechanism is via the process $f + \overline{f} \to X_1 + X_2$ followed by the radiative decay $X_2 \to X_1 + \gamma$, if X_2 is short-lived. The cross section is of order $\sigma(f + \overline{f} \to X_1 + X_2) \approx 10^{10}\,\text{fb} \times (1\,\text{GeV}/\Lambda)^4$ for $e^+ e^-$ collisions at a center-of-mass energy of $10\,\text{GeV}$. For $\Lambda \sim 10^4\,\text{GeV}$, typical values for Λ in this region of parameter space, the production rate is too small to be constrained by existing analyses. However, it may be visible in future searches at Belle II [70].

The above conclusions are a general feature of freeze-in scenarios, where the reaction cross sections required to produce the observed dark matter abundance are small, making them very difficult to detect experimentally.

4 Conclusions

We have presented general extensions of the SMEFT and the LEFT by adding spin 0, 1/2 and 1 particles to the two theories, where the additional particles are singlets under the SM gauge group. We have classified all operators up to dimension-six which involve the new particles, including those which violate baryon and/or lepton number. We have also computed the tree-level matching at the electroweak scale between the two dark matter theories.

An interesting example is the case of vector dark matter with a discrete $\mathbb{Z}_2$ symmetry, where the lightest dark matter particle is stable. Our operator analysis shows that the interaction with SM particles in this case is via a dimension-six triple gauge boson interaction. We have made a preliminary analysis of the phenomenology of this model, and showed that there are regions of parameter space where the freeze-in scenario is viable.

Acknowledgments

A   Purely dark matter operators

In this appendix we list all the self-interactions among the three different DM particles listed in table 1 up to dimension six. The generation indices of the DM fields a, b, c, d

run over n_ϕ scalars, n_χ fermions, and n_X gauge bosons. The results in this appendix also give the possible interactions up to dimension six in a general gauge theory (with the replacement of derivatives by covariant derivatives). The possible interactions are restricted by the symmetries of the theory.

The operators range from the dimension-one operator $\mathcal{P}_\phi = \phi_a$, containing only one scalar field ϕ up to dimension six. We have chosen to retain the linear term in ϕ_a, rather than shifting the scalar fields to remove the linear term, to avoid complicated expressions for the matching. In many examples, a linear ϕ_a term is forbidden by symmetry. We have also chosen to include the DM kinetic energy terms in the list of dimension-four operators. These terms are usually canonically normalized. Here, integrating out particles at the electroweak scale gives a matching contribution to the DM kinetic energy terms for X_μ. Rather than rescale the DM fields to get a canonically normalized kinetic term, which changes all the operator coefficients, we have instead included the matching in table 2.

We have given the number of operators of a given type in the tables. In most examples, the counting of operators is trivial. For example, the number of $\phi_a \phi_b \phi_c \phi_d$ operators is $n_\phi(n_\phi+1)(n_\phi+2)(n_\phi+3)/4!$, because the operator is symmetric in a, b, c, d. In two cases, the counting is non-trivial. The dimension-six operator with two derivatives and four scalar fields has the form $\mathcal{P}_{\partial^2\phi^4 \atop abcd} = \partial_\mu \phi^a \partial^\mu \phi_b \phi_c \phi_d$, which is symmetric in a, b and in c, d. $\mathcal{P}_{\partial^2\phi^4 \atop abcd}$ then transforms as

$$\square\square \otimes \square\square = \square\square\square\square \oplus \begin{array}{c}\square\square\square\\\square\end{array} \oplus \begin{array}{c}\square\square\\\square\square\end{array} \tag{A.1}$$

under the permutation group. However, total derivatives do not contribute to the action, so that

$$\partial_\mu(\partial^\mu \phi_a \phi_b \phi_c \phi_d) = \partial^2 \phi_a \phi_b \phi_c \phi_d + \partial^\mu \phi_a \partial_\mu \phi_b \phi_c \phi_d + \partial^\mu \phi_a \phi_b \partial_\mu \phi_c \phi_d + \partial^\mu \phi_a \phi_b \phi_c \partial_\mu \phi_d \,, \tag{A.2}$$

can be set to zero. $\partial^2 \phi_a$ can be eliminated by a field-redefinition (i.e. the equations of motion), so that $\partial^\mu \phi_a \partial_\mu \phi_b \phi_c \phi_d + \partial^\mu \phi_a \phi_b \partial_\mu \phi_c \phi_d + \partial^\mu \phi_a \phi_b \phi_c \partial_\mu \phi_d \to 0$ in the action. As a result, the part of $\mathcal{P}_{\partial^2\phi^4 \atop abcd}$ symmetric in three indices vanishes, and $\mathcal{P}_{\partial^2\phi^4 \atop abcd}$ transforms as

$$\mathcal{P}_{\partial^2\phi^4 \atop abcd} \sim \begin{array}{c}\square\square\\\square\square\end{array} \tag{A.3}$$

under the permutation group, and has dimension

$$\frac{1}{12} n_\phi^2 (n_\phi^2 - 1) \,. \tag{A.4}$$

For fermions, there is a Fierz identity

$$(\chi_a^T C \chi_b)(\chi_c^T C \chi_d) + (\chi_a^T C \chi_c)(\chi_d^T C \chi_b) + (\chi_a^T C \chi_d)(\chi_b^T C \chi_c) = 0 \,, \tag{A.5}$$

so that $\mathcal{P}_{\chi\chi}$ in table 7 transforms as in eq. (A.3) and has dimension given in eq. (A.4) with $n_\phi \to n_\chi$.

In the matching the vacuum expectation value v_T appears, given by [71–73]

$$v_T = \left(1 + \frac{3}{8\lambda}C_H v^2\right) v\,. \tag{A.6}$$

Furthermore, we use the notation

$$\binom{a}{b} \equiv \frac{a!}{b!(a-b)!} \tag{A.7}$$

for the binomial coefficient. Note that the DM operators in tables 2–7 are present both in DSMEFT and DLEFT, so what is shown in the tables is the *shift* in the coefficients when electroweak scale particles are integrated out. For example, for the $\mathcal{P}_{\phi^4}$ operator in table 5, the coefficient below the EW scale is

$$C^{\text{DLEFT}}_{\phi^4} = C^{\text{DSMEFT}}_{\phi^4} + \frac{v_T^2}{2}C_{H^2\phi^4}\,. \tag{A.8}$$
$$\quad{}_{abcd}\qquad\quad{}_{abcd}\qquad\qquad{}_{abcd}$$

Only the second term is given in table 5.

DM: dimension 1

$(d_{\text{SM}}, d_{\text{DM}})$	Name	Operator	Number	Matching
$(0,1)$	$\mathcal{P}_\phi$	ϕ_a	n_ϕ	$\frac{v_T^2}{2}\left(C_{H^2\phi}_{\,a} + \frac{v_T^2}{2}C_{H^4\phi}_{\,a}\right)$

Table 2. Dimension-one purely DM operator present in DSMEFT and DLEFT. The first column gives the dimensions of the SM and DM part of the operator, the fourth column is the number of operators, and the fifth column is the *additional* matching contribution at the EW scale.

DM: dimension 2

$(d_{\text{SM}}, d_{\text{DM}})$	Name	Operator	Number	Matching
$(0,2)$	$\mathcal{P}_{\phi^2}$	$\phi_a\phi_b$	$\binom{n_\phi+1}{2}$	$\frac{v_T^2}{2}\left(C_{H^2\phi^2}_{\,ab} + \frac{v_T^2}{2}C_{H^4\phi^2}_{\,ab}\right)$

Table 3. Dimension-two purely DM operator present in DSMEFT and DLEFT. The first column gives the dimensions of the SM and DM part of the operator, the fourth column is the number of operators, and the fifth column is the *additional* matching contribution at the EW scale. This operator is the ϕ mass term.

DM: dimension 3

$(d_{\text{SM}}, d_{\text{DM}})$	Name	Operator	Number	Matching
$(0,3)$	$\mathcal{P}_{\phi^3}$	$\phi_a\phi_b\phi_c$	$\binom{n_\phi+2}{3}$	$\frac{v_T^2}{2}C_{H^2\phi^3}_{\,abc}$
	$\mathcal{P}_\chi$	$(\chi_a^T C \chi_b)$ + h.c.	$\binom{n_\chi+1}{2}$ + h.c.	$\frac{v_T^2}{2}C_{H\chi}_{\,ab}$

Table 4. Dimension-three purely DM operators present in DSMEFT and DLEFT. The first column gives the dimensions of the SM and DM part of the operator, the fourth column is the number of operators, and the fifth column is the *additional* matching contribution at the EW scale. $\mathcal{P}_\chi$ is the χ mass term.

DM: dimension 4

(d_{SM}, d_{DM})	Name	Operator	Number	Matching
	$\mathcal{P}_\phi^{\mathrm{kin}}$	$\partial_\mu \phi_a \partial^\mu \phi_b$	$\binom{n_\phi+1}{2}$	0
	$\mathcal{P}_\chi^{\mathrm{kin}}$	$\overline{\chi}_a\, i\slashed{\partial}\, \chi_b$	$\binom{n_\chi+1}{2}$	0
	$\mathcal{P}_X^{\mathrm{kin}}$	$X_{a\,\mu\nu} X_b^{\mu\nu}$	$\binom{n_X+1}{2}$	$\frac{v_T^2}{2} C_{HX\atop ab}$
$(0,4)$	$\mathcal{P}_{\widetilde{X}}$	$\widetilde{X}_{a\,\mu\nu} X_b^{\mu\nu}$	$\binom{n_X}{2}$	$\frac{v_T^2}{2} C_{H\widetilde{X}\atop ab}$
	$\mathcal{P}_{\phi^4}$	$\phi_a\phi_b\phi_c\phi_d$	$\binom{n_\phi+3}{4}$	$\frac{v_T^2}{2} C_{H^2\phi^4\atop abcd}$
	$\mathcal{P}_{\chi\phi}$	$(\chi_a^T C\chi_b)\phi_c$ + h.c.	$n_\phi \binom{n_\chi+1}{2}$ + h.c.	$\frac{v_T^2}{2} C_{H\chi\phi\atop abc}$

Table 5. Dimension-four purely DM operators present in DSMEFT and DLEFT. The first column gives the dimensions of the SM and DM part of the operator, the fourth column is the number of operators, and the fifth column is the *additional* matching contribution at the EW scale. The first three operators are the DM kinetic energy terms.

DM: dimension 5

(d_{SM}, d_{DM})	Name	Operator	Number	Matching
	$\mathcal{P}_{\phi^5}$	$\phi_a\phi_b\phi_c\phi_d\phi_e$	$\binom{n_\phi+4}{5}$	0
	$\mathcal{P}_{X\phi}$	$X_{a\,\mu\nu} X_b^{\mu\nu} \phi_c$	$n_\phi \binom{n_X+1}{2}$	0
$(0,5)$	$\mathcal{P}_{\widetilde{X}\phi}$	$\widetilde{X}_{a\,\mu\nu} X_b^{\mu\nu} \phi_c$	$n_\phi \binom{n_X+1}{2}$	0
	$\mathcal{P}_{\chi\phi^2}$	$(\chi_a^T C\chi_b)\phi_c\phi_d$ + h.c.	$\binom{n_\phi+1}{2}\binom{n_\chi+1}{2}$ + h.c.	0
	$\mathcal{P}_{\chi X}$	$(\chi_a^T C\sigma^{\mu\nu}\chi_b)X_{c\,\mu\nu}$ + h.c.	$\binom{n_\chi}{2}n_X$ + h.c.	0

Table 6. Dimension-five purely DM operators present in DSMEFT and DLEFT. The first column gives the dimensions of the SM and DM part of the operator, the fourth column is the number of operators, and the fifth column is the *additional* matching contribution at the EW scale.

DM: dimension 6

(d_{SM}, d_{DM})	Name	Operator	Number	Matching
	$\mathcal{P}_{X^3}$	$X_{a\,\mu}{}^\nu X_{b\,\nu}{}^\alpha X_{c\,\alpha}{}^\mu$	$\binom{n_X}{3}$	0
	$\mathcal{P}_{\widetilde{X}^3}$	$\widetilde{X}_{a\,\mu}{}^\nu X_{b\,\nu}{}^\alpha X_{c\,\alpha}{}^\mu$	$\binom{n_X}{3}$	0
	$\mathcal{P}_{X\phi^2}$	$X_{a\,\mu\nu} X_b^{\mu\nu}\phi_c\phi_d$	$\binom{n_\phi+1}{2}\binom{n_X+1}{2}$	0
	$\mathcal{P}_{\widetilde{X}\phi^2}$	$\widetilde{X}_{a\,\mu\nu} X_b^{\mu\nu}\phi_c\phi_d$	$\binom{n_\phi+1}{2}\binom{n_X+1}{2}$	0
	$\mathcal{P}_{\phi^6}$	$\phi_a\phi_b\phi_c\phi_d\phi_e\phi_f$	$\binom{n_\phi+5}{6}$	0
$(0,6)$	$\mathcal{P}_{\partial^2\phi^4}$	$\partial_\mu \phi_a \partial^\mu \phi_b \phi_c \phi_d$	$\frac{1}{12}n_\phi^2(n_\phi^2-1)$	$\frac{\overline{g}_Z^2}{4M_Z^2}([Z_\phi]_{ac}-[Z_\phi]_{ca})([Z_\phi]_{bd}-[Z_\phi]_{db})$
				$+\, a \leftrightarrow b$
	$\mathcal{P}_{\chi\phi^3}$	$(\chi_a^T C\chi_b)\phi_c\phi_d\phi_e$ + h.c.	$\binom{n_\phi+2}{3}\binom{n_\chi+1}{2}$ + h.c.	0
	$\mathcal{P}_{\chi X\phi}$	$(\chi_a^T C\sigma^{\mu\nu}\chi_b)X_{c\,\mu\nu}\phi_d$ + h.c.	$n_\phi\binom{n_\chi}{2}n_X$ + h.c.	0
	$\mathcal{P}_{\chi\partial\phi}$	$(\overline{\chi}_a\gamma_\mu\chi_b)(i\phi_c\overset{\leftrightarrow}{\partial^\mu}\phi_d)$	$\binom{n_\phi}{2}n_\chi^2$	$-\frac{\overline{g}_Z^2}{M_Z^2}[Z_\chi]_{ab}[Z_\phi]_{cd}$
	$\mathcal{P}_{\chi\chi}$	$(\chi_a^T C\chi_b)(\chi_c^T C\chi_d)$ + h.c.	$\frac{1}{12}n_\chi^2(n_\chi^2-1)$ + h.c.	0
	$\mathcal{P}_{\chi\overline{\chi}}$	$(\chi_a^T C\chi_b)(\overline{\chi}_c C\overline{\chi}_d^T)$	$\binom{n_\chi+1}{2}\binom{n_\chi+1}{2}$	$-\frac{\overline{g}_Z^2}{M_Z^2}[Z_\chi]_{ca}[Z_\chi]_{db}-\frac{\overline{g}_Z^2}{M_Z^2}[Z_\chi]_{cb}[Z_\chi]_{da}$

Table 7. Dimension-six purely DM operators present in DSMEFT and DLEFT. The first column gives the dimensions of the SM and DM part of the operator, the fourth column is the number of operators, and the fifth column is the *additional* matching contribution at the EW scale.

B DSMEFT operators

This appendix gives the operators up to dimension six in DSMEFT which have both SM and DM fields. The purely DM operators are given in appendix A, and the purely SMEFT operators in ref. [46]. Following the notation in [46], we denote the generation indices of the SM fields by p, r, s, t and the number of generations by n_g. The subset of operators containing SM fields and a right-handed neutrino has already been studied extensively in the literature. Theories with this field content are called νSMEFT or SMNEFT and have been discussed for instance in refs. [74–79]. For this subset of operators, most of the one-loop RG running is known. The gauge mixing is presented in [80], mixing among bosonic operators is discussed in [81], the one-loop RGE of the four-fermion operators is provided in [82] and the Yukawa mixing for four-fermion operators is computed recently in [83].

It is assumed that all dark matter particles have baryon number $B = 0$ and lepton number $L = 0$ when we give the ΔB and ΔL quantum numbers of the operators. Note that if χ is a right-handed sterile neutrino, $L = 1$, and the lepton number assignments of all the operators get shifted by the number of χ fields.

DSMEFT: dimension 3 $\Delta B = \Delta L = 0$

$(\mathrm{d_{SM}}, \mathrm{d_{DM}})$	Name	Operator	Number
$(2,1)$	$\mathcal{Q}_{H^2\phi}$	$(H^\dagger H)\phi_a$	n_ϕ

Table 8. Dimension-three $\Delta B = \Delta L = 0$ operator in DSMEFT. The first column gives the dimensions of the SM and DM part of the operator, and the fourth column is the number of operators.

DSMEFT: dimension 4 $\Delta B = \Delta L = 0$

$(\mathrm{d_{SM}}, \mathrm{d_{DM}})$	Name	Operator	Number
$(2,2)$	$\mathcal{Q}_{BX}$	$B_{\mu\nu}X_a^{\mu\nu}$	n_X
	$\mathcal{Q}_{\widetilde{B}X}$	$\widetilde{B}_{\mu\nu}X_a^{\mu\nu}$	n_X
	$\mathcal{Q}_{H^2\phi^2}$	$(H^\dagger H)\phi_a\phi_b$	$\binom{n_\phi+1}{2}$

Table 9. Dimension-four $\Delta B = \Delta L = 0$ operators in DSMEFT. The first column gives the dimensions of the SM and DM part of the operator, and the fourth column is the number of operators.

DSMEFT: dimension 5		$\Delta B = \Delta L = 0$	
$(\mathrm{d_{SM}}, \mathrm{d_{DM}})$	Name	Operator	Number
(2,3)	$\mathcal{Q}_{H^2\phi^3}$	$(H^\dagger H)\phi_a\phi_b\phi_c$	$\binom{n_\phi+2}{3}$
	$\mathcal{Q}_{BX\phi}$	$B_{\mu\nu}X_a^{\mu\nu}\phi_b$	$n_\phi n_X$
	$\mathcal{Q}_{\widetilde{B}X\phi}$	$\widetilde{B}_{\mu\nu}X_a^{\mu\nu}\phi_b$	$n_\phi n_X$
	$\mathcal{Q}_{H\chi}$	$(H^\dagger H)(\chi_a^T C \chi_b)$ + h.c.	$\binom{n_\chi+1}{2}$ + h.c.
	$\mathcal{Q}_{B\chi}$	$B_{\mu\nu}(\chi_a^T C \sigma^{\mu\nu}\chi_b)$ + h.c.	$\binom{n_\chi}{2}$ + h.c.
(4,1)	$\mathcal{Q}_{H^4\phi}$	$(H^\dagger H)^2\phi_a$	n_ϕ
	$\mathcal{Q}_{B\phi}$	$B_{\mu\nu}B^{\mu\nu}\phi_a$	n_ϕ
	$\mathcal{Q}_{\widetilde{B}\phi}$	$\widetilde{B}_{\mu\nu}B^{\mu\nu}\phi_a$	n_ϕ
	$\mathcal{Q}_{W\phi}$	$W^I_{\mu\nu}W^{I\,\mu\nu}\phi_a$	n_ϕ
	$\mathcal{Q}_{\widetilde{W}\phi}$	$\widetilde{W}^I_{\mu\nu}W^{I\,\mu\nu}\phi_a$	n_ϕ
	$\mathcal{Q}_{G\phi}$	$G^A_{\mu\nu}G^{A\,\mu\nu}\phi_a$	n_ϕ
	$\mathcal{Q}_{\widetilde{G}\phi}$	$\widetilde{G}^A_{\mu\nu}G^{A\,\mu\nu}\phi_a$	n_ϕ
	$\mathcal{Q}_{e\phi}$	$(\bar{l}_p e_r H)\phi_a$ + h.c.	$n_g^2 n_\phi$ + h.c.
	$\mathcal{Q}_{u\phi}$	$(\bar{q}_p u_r \widetilde{H})\phi_a$ + h.c.	$n_g^2 n_\phi$ + h.c.
	$\mathcal{Q}_{d\phi}$	$(\bar{q}_p d_r H)\phi_a$ + h.c.	$n_g^2 n_\phi$ + h.c.

Table 10. Dimension-five $\Delta B = \Delta L = 0$ operators in DSMEFT. The first column gives the dimensions of the SM and DM part of the operator, and the fourth column is the number of operators.

DSMEFT: dimension 6		$\Delta B = \Delta L = 0$	
$(\mathrm{d_{SM}}, \mathrm{d_{DM}})$	Name	Operator	Number
(2,4)	$\mathcal{Q}_{BX^2}$	$B_\mu{}^\nu X_{a\,\nu}{}^\alpha X_{b\,\alpha}{}^\mu$	$\binom{n_X}{2}$
	$\mathcal{Q}_{\widetilde{B}X^2}$	$\widetilde{B}_\mu{}^\nu X_{a\,\nu}{}^\alpha X_{b\,\alpha}{}^\mu$	$\binom{n_X}{2}$
	$\mathcal{Q}_{BX\phi^2}$	$B_{\mu\nu}X_a^{\mu\nu}\phi_b\phi_c$	$\binom{n_\phi+1}{2}n_X$
	$\mathcal{Q}_{\widetilde{B}X\phi^2}$	$\widetilde{B}_{\mu\nu}X_a^{\mu\nu}\phi_b\phi_c$	$\binom{n_\phi+1}{2}n_X$
	$\mathcal{Q}_{HX}$	$(H^\dagger H)X_{a\,\mu\nu}X_b^{\mu\nu}$	$\binom{n_X+1}{2}$
	$\mathcal{Q}_{H\widetilde{X}}$	$(H^\dagger H)\widetilde{X}_{a\,\mu\nu}X_b^{\mu\nu}$	$\binom{n_X+1}{2}$
	$\mathcal{Q}_{H^2\phi^4}$	$(H^\dagger H)\phi_a\phi_b\phi_c\phi_d$	$\binom{n_\phi+3}{4}$
	$\mathcal{Q}_{H\chi\phi}$	$(H^\dagger H)(\chi_a^T C \chi_b)\phi_c$ + h.c.	$n_\phi\binom{n_\chi+1}{2}$ + h.c.
	$\mathcal{Q}_{B\chi\phi}$	$B_{\mu\nu}(\chi_a^T C \sigma^{\mu\nu}\chi_b)\phi_c$ + h.c.	$n_\phi\binom{n_\chi}{2}$ + h.c.
(3,3)	$\mathcal{Q}_{\partial H\partial\phi}$	$\partial^\mu(H^\dagger H)\partial_\mu(\phi_a\phi_b)$	$\binom{n_\phi+1}{2}$
	$\mathcal{Q}_{DH\partial\phi}$	$(H^\dagger \overleftrightarrow{D}^\mu H)(\phi_a \overleftrightarrow{\partial}_\mu \phi_b)$	$\binom{n_\phi}{2}$
	$\mathcal{Q}_{DH\chi}$	$(iH^\dagger \overleftrightarrow{D}^\mu H)(\overline{\chi}_a\gamma_\mu\chi_b)$	n_χ^2
	$\mathcal{Q}_{\phi l}$	$(\bar{l}_p\gamma_\mu l_r)(i\phi_a\overleftrightarrow{\partial}^\mu\phi_b)$	$n_g^2\binom{n_\phi}{2}$
	$\mathcal{Q}_{\phi q}$	$(\bar{q}_p\gamma_\mu q_r)(i\phi_a\overleftrightarrow{\partial}^\mu\phi_b)$	$n_g^2\binom{n_\phi}{2}$
	$\mathcal{Q}_{\phi e}$	$(\bar{e}_p\gamma_\mu e_r)(i\phi_a\overleftrightarrow{\partial}^\mu\phi_b)$	$n_g^2\binom{n_\phi}{2}$
	$\mathcal{Q}_{\phi u}$	$(\bar{u}_p\gamma_\mu u_r)(i\phi_a\overleftrightarrow{\partial}^\mu\phi_b)$	$n_g^2\binom{n_\phi}{2}$
	$\mathcal{Q}_{\phi d}$	$(\bar{d}_p\gamma_\mu d_r)(i\phi_a\overleftrightarrow{\partial}^\mu\phi_b)$	$n_g^2\binom{n_\phi}{2}$
	$\mathcal{Q}_{l\chi}$	$(\bar{l}_p\gamma_\mu l_r)(\overline{\chi}_a\gamma^\mu\chi_b)$	$n_g^2 n_\chi^2$
	$\mathcal{Q}_{q\chi}$	$(\bar{q}_p\gamma_\mu q_r)(\overline{\chi}_a\gamma^\mu\chi_b)$	$n_g^2 n_\chi^2$
	$\mathcal{Q}_{e\chi}$	$(\bar{e}_p\gamma_\mu e_r)(\overline{\chi}_a\gamma^\mu\chi_b)$	$n_g^2 n_\chi^2$
	$\mathcal{Q}_{u\chi}$	$(\bar{u}_p\gamma_\mu u_r)(\overline{\chi}_a\gamma^\mu\chi_b)$	$n_g^2 n_\chi^2$
	$\mathcal{Q}_{d\chi}$	$(\bar{d}_p\gamma_\mu d_r)(\overline{\chi}_a\gamma^\mu\chi_b)$	$n_g^2 n_\chi^2$

Table 11. Dimension-six $\Delta B = \Delta L = 0$ operators in DSMEFT, part 1. The first column gives the dimensions of the SM and DM part of the operator, and the fourth column is the number of operators.

DSMEFT: dimension 6		$\Delta B = \Delta L = 0$	
$(\mathrm{d}_{SM}, \mathrm{d}_{DM})$	Name	Operator	Number
(4,2)	$\mathcal{Q}_{H^4\phi^2}$	$(H^\dagger H)^2 \phi_a \phi_b$	$\binom{n_\phi+1}{2}$
	$\mathcal{Q}_{B\phi^2}$	$B_{\mu\nu} B^{\mu\nu} \phi_a \phi_b$	$\binom{n_\phi+1}{2}$
	$\mathcal{Q}_{\widetilde{B}\phi^2}$	$\widetilde{B}_{\mu\nu} B^{\mu\nu} \phi_a \phi_b$	$\binom{n_\phi+1}{2}$
	$\mathcal{Q}_{W\phi^2}$	$W^I_{\mu\nu} W^{I\,\mu\nu} \phi_a \phi_b$	$\binom{n_\phi+1}{2}$
	$\mathcal{Q}_{\widetilde{W}\phi^2}$	$\widetilde{W}^I_{\mu\nu} W^{I\,\mu\nu} \phi_a \phi_b$	$\binom{n_\phi+1}{2}$
	$\mathcal{Q}_{G\phi^2}$	$G^A_{\mu\nu} G^{A\,\mu\nu} \phi_a \phi_b$	$\binom{n_\phi+1}{2}$
	$\mathcal{Q}_{\widetilde{G}\phi^2}$	$\widetilde{G}^A_{\mu\nu} G^{A\,\mu\nu} \phi_a \phi_b$	$\binom{n_\phi+1}{2}$
	$\mathcal{Q}_{H^2 B X}$	$(H^\dagger H) B_{\mu\nu} X_a^{\mu\nu}$	n_X
	$\mathcal{Q}_{H^2 \widetilde{B} X}$	$(H^\dagger H) \widetilde{B}_{\mu\nu} X_a^{\mu\nu}$	n_X
	$\mathcal{Q}_{H^2 W X}$	$(H^\dagger \tau^I H) W^I_{\mu\nu} X_a^{\mu\nu}$	n_X
	$\mathcal{Q}_{H^2 \widetilde{W} X}$	$(H^\dagger \tau^I H) \widetilde{W}^I_{\mu\nu} X_a^{\mu\nu}$	n_X
	$\mathcal{Q}_{e\phi^2}$	$(\bar{l}_p e_r H) \phi_a \phi_b + \text{h.c.}$	$n_g^2 \binom{n_\phi+1}{2} + \text{h.c.}$
	$\mathcal{Q}_{u\phi^2}$	$(\bar{q}_p u_r \widetilde{H}) \phi_a \phi_b + \text{h.c.}$	$n_g^2 \binom{n_\phi+1}{2} + \text{h.c.}$
	$\mathcal{Q}_{d\phi^2}$	$(\bar{q}_p d_r H) \phi_a \phi_b + \text{h.c.}$	$n_g^2 \binom{n_\phi+1}{2} + \text{h.c.}$
	$\mathcal{Q}_{eX}$	$(\bar{l}_p \sigma_{\mu\nu} e_r) H X_a^{\mu\nu} + \text{h.c.}$	$n_g^2 n_X + \text{h.c.}$
	$\mathcal{Q}_{uX}$	$(\bar{q}_p \sigma_{\mu\nu} u_r) \widetilde{H} X_a^{\mu\nu} + \text{h.c.}$	$n_g^2 n_X + \text{h.c.}$
	$\mathcal{Q}_{dX}$	$(\bar{q}_p \sigma_{\mu\nu} d_r) H X_a^{\mu\nu} + \text{h.c.}$	$n_g^2 n_X + \text{h.c.}$

Table 12. Dimension-six $\Delta B = \Delta L = 0$ operators in DSMEFT, part 2. The first column gives the dimensions of the SM and DM part of the operator, and the fourth column is the number of operators.

DSMEFT: dimension 4 $\Delta B = 0$, $\Delta L = 1 + \text{h.c.}$			
$(\mathrm{d}_{SM}, \mathrm{d}_{DM})$	Name	Operator	Number
$(5/2, 3/2)$	$\mathcal{Q}_{H\chi l}$	$\left\| \epsilon_{ij} H^i (\bar{\chi}_a l_p^j) \right\|$	$n_g n_\chi$

Table 13. Dimension-four $\Delta B = 0$, $\Delta L = 1$ operator in DSMEFT. The first column gives the dimensions of the SM and DM part of the operator, and the fourth column is the number of operators.

DSMEFT: dimension 5 $\Delta B = 0$, $\Delta L = 1 + \text{h.c.}$			
$(\mathrm{d}_{SM}, \mathrm{d}_{DM})$	Name	Operator	Number
$(5/2, 5/2)$	$\mathcal{Q}_{H\chi l\phi}$	$\left\| \epsilon_{ij} H^i (\bar{\chi}_a l_p^j) \phi_b \right\|$	$n_g n_\phi n_\chi$

Table 14. Dimension-five $\Delta B = 0$, $\Delta L = 1$ operator in DSMEFT. The first column gives the dimensions of the SM and DM part of the operator, and the fourth column is the number of operators.

	DSMEFT: dimension 6		**$\Delta B = 0, \ \Delta L = 1 +$ h.c.**	
$(\mathrm{d_{SM}}, \mathrm{d_{DM}})$	Name		Operator	Number
(5/2,7/2)	$\mathcal{Q}_{H\chi l\phi^2}$		$\epsilon_{ij}H^i(\overline{\chi}_a l_p^{lj})\phi_b\phi_c$	$n_g\binom{n_\phi+1}{2}n_\chi$
	$\mathcal{Q}_{H\chi l\partial\phi}$		$\epsilon_{ij}H^i(\chi_a^T C\gamma_\mu l_p^j)\partial^\mu\phi_b$	$n_g n_\phi n_\chi$
	$\mathcal{Q}_{H\chi lX}$		$\epsilon_{ij}H^i(\overline{\chi}_a\sigma^{\mu\nu}l_p^j)X_{b\,\mu\nu}$	$n_g n_\chi n_X$
(9/2,3/2)	$\mathcal{Q}_{H^3\chi l}$		$\epsilon_{ij}H^i(H^\dagger H)(\overline{\chi}_a l_p^j)$	$n_g n_\chi$
	$\mathcal{Q}_{H\chi e}$		$(i\widetilde{H}^\dagger D^\mu H)(\overline{\chi}_a\gamma_\mu e_p)$	$n_g n_\chi$
	$\mathcal{Q}_{HB\chi l}$		$\epsilon_{ij}H^j B_{\mu\nu}(\overline{\chi}_a\sigma^{\mu\nu}l_p^i)$	$n_g n_\chi$
	$\mathcal{Q}_{HW\chi l}$		$\epsilon_{ik}(\tau^I)^k{}_j H^j W_{\mu\nu}^I(\overline{\chi}_a\sigma^{\mu\nu}l_p^i)$	$n_g n_\chi$
	$\mathcal{Q}_{le\chi}^{(1)}$		$\epsilon_{ij}(l_p^{i\,T}Cl_r^j)(\overline{e}_s C\overline{\chi}_a^T)$	$n_g\binom{n_g}{2}n_\chi$
	$\mathcal{Q}_{le\chi}^{(3)}$		$\epsilon_{ij}(l_p^{i\,T}C\sigma^{\mu\nu}l_r^j)(\overline{e}_s\sigma_{\mu\nu}C\overline{\chi}_a^T)$	$n_g\binom{n_g+1}{2}n_\chi$
	$\mathcal{Q}_{dq\chi l}^{(1)}$		$\epsilon_{ij}(\overline{d}_p q_r^i)(\overline{\chi}_a l_s^j)$	$n_g^3 n_\chi$
	$\mathcal{Q}_{dq\chi l}^{(3)}$		$\epsilon_{ij}(\overline{d}_p\sigma_{\mu\nu}q_r^i)(\overline{\chi}_a\sigma^{\mu\nu}l_s^j)$	$n_g^3 n_\chi$
	$\mathcal{Q}_{du\chi e}$		$(\overline{d}_p\gamma_\mu u_r)(\overline{\chi}_a\gamma^\mu e_s)$	$n_g^3 n_\chi$
	$\mathcal{Q}_{qu\chi l}$		$(\overline{q}_p^i u_r)(\overline{\chi}_a l_s^i)$	$n_g^3 n_\chi$

Table 15. Dimension-six $\Delta B = 0$, $\Delta L = 1$ operators in DSMEFT. The first column gives the dimensions of the SM and DM part of the operator, and the fourth column is the number of operators.

	DSMEFT: dimension 6		**$\Delta B = 0, \ \Delta L = 2 +$ h.c.**	
$(\mathrm{d_{SM}}, \mathrm{d_{DM}})$	Name		Operator	Number
(5,1)	$\mathcal{Q}_{\nu\nu\phi}$		$\epsilon_{ij}\epsilon_{kl}H^j H^l(l_p^{i\,T}Cl_r^k)\phi_a$	$\binom{n_g+1}{2}n_\phi$

Table 16. Dimension-six $\Delta B = 0$, $\Delta L = 2$ operator in DSMEFT. The first column gives the dimensions of the SM and DM part of the operator, and the fourth column is the number of operators.

	DSMEFT: dimension 6		**$\Delta L = 0, \ \Delta B = 1 +$ h.c.**	
$(\mathrm{d_{SM}}, \mathrm{d_{DM}})$	Name		Operator	Number
(9/2,3/2)	$\mathcal{Q}_{ddu}^{(1)}$		$\epsilon^{\alpha\beta\gamma}(d_p^{\alpha\,T}Cd_r^\beta)(\chi_a^T Cu_s^\gamma)$	$n_g\binom{n_g}{2}n_\chi$
	$\mathcal{Q}_{ddu}^{(3)}$		$\epsilon^{\alpha\beta\gamma}(d_p^{\alpha\,T}C\sigma_{\mu\nu}d_r^\beta)(\chi_a^T C\sigma^{\mu\nu}u_s^\gamma)$	$n_g\binom{n_g+1}{2}n_\chi$
	$\mathcal{Q}_{qqd}$		$\epsilon^{\alpha\beta\gamma}\epsilon_{ij}(q_p^{i\alpha\,T}Cq_r^{j\beta})(\chi_a^T Cd_s^\gamma)$	$n_g\binom{n_g+1}{2}n_\chi$

Table 17. Dimension-six $\Delta L = 0$, $\Delta B = 1$ operators in DSMEFT. The first column gives the dimensions of the SM and DM part of the operator, and the fourth column is the number of operators.

C DLEFT operators

This appendix gives the DLEFT operators up to dimension six that include both DM and LEFT fields. The purely DM operators are given in appendix A and the purely LEFT operators in [47, 48]. We also give the tree-level matching contributions to these operators from DSMEFT, when heavy SM degrees of freedom are integrated out at the EW scale. The matching conditions depend on the $\mathcal{Z}$ and $\mathcal{W}$ couplings

$$[Z_\phi]_{ab} = \frac{1}{2}v_T^2\, C_{DH\partial\phi\atop ab}\,, \qquad [Z_\chi]_{ab} = -\frac{1}{2}v_T^2\, C_{DH\chi\atop ab}\,, \qquad [W_\chi]_{ap} = \frac{1}{2}v_T^2\, C_{H\chi e\atop ap}\,, \tag{C.1}$$

and

$$A_{BW} = v_T^2\,\overline{s}\, C_{H^2BX} + v_T^2\,\overline{c}\, C_{H^2WX} + 2\overline{s}C_{BX}\,, \tag{C.2}$$

$$A_{\widetilde{BW}} = v_T^2\,\overline{s}\, C_{H^2\widetilde{B}X} + v_T^2\,\overline{c}\, C_{H^2\widetilde{W}X} + 2\overline{s}C_{\widetilde{B}X}\,, \tag{C.3}$$

The neutral and charged currents are

$$J^\mu = A_{BW}\partial_\nu X^{\nu\mu} + A_{\widetilde{BW}}\partial_\nu \widetilde{X}^{\nu\mu}, \tag{C.4}$$

$$\begin{aligned} j_Z^\mu &= [Z_\phi]_{ab}(i\phi_a\overset{\leftrightarrow}{\partial^\mu}\phi_b) + [Z_\chi]_{ab}(\overline{\chi}_a\gamma^\mu\chi_b) + [Z_{\nu_L}]_{pr}(\overline{\nu}_{Lp}\gamma^\mu\nu_{Ls}) + [Z_{e_L}]_{pr}(\overline{e}_{Lp}\gamma^\mu e_{Lr}) \\ &\quad + [Z_{e_R}]_{pr}(\overline{e}_{Rp}\gamma^\mu e_{Rr}) + [Z_{u_L}]_{pr}(\overline{u}_{Lp}\gamma^\mu u_{Lr}) + [Z_{u_R}]_{pr}(\overline{u}_{Rp}\gamma^\mu u_{Rr}) + [Z_{d_L}]_{pr}(\overline{d}_{Lp}\gamma^\mu d_{Lr}) \\ &\quad + [Z_{d_R}]_{pr}(\overline{d}_{Rp}\gamma^\mu d_{Rr})\,, \end{aligned} \tag{C.5}$$

$$j_W^\mu = [W_\chi]_{ap}(\overline{\chi}_a\gamma^\mu e_p) + [W_l]_{pr}(\overline{\nu}_{Lp}\gamma^\mu e_{Lr}) + [W_q]_{pr}(\overline{u}_{Lp}\gamma^\mu d_{Lr}) + [W_R]_{pr}(\overline{u}_{Rp}\gamma^\mu d_{Rr})\,, \tag{C.6}$$

which enter the interaction Lagrangian

$$\mathcal{L} = -\mathcal{Z}_\mu\left(\overline{g}_Z j_Z^\mu + J^\mu\right) - \frac{\overline{g}_2}{\sqrt{2}}\left(\mathcal{W}_\mu^+ j_W^\mu + \text{h.c.}\right) + \ldots\,. \tag{C.7}$$

The relation of the mass eigenstate fields $\mathcal{Z}$ and $\mathcal{W}$ to the electroweak fields W^3 and B as well as the couplings $[Z_{f_i}]_{pr}$ for SM fermions are defined in [47]. The couplings $\overline{g}_Z$ and $\overline{g}_W$ are defined in ref. [73]. Integrating out the $\mathcal{Z}$ and $\mathcal{W}$ fields give the low-energy interaction

$$\mathcal{L} = -\frac{\overline{g}_2^2}{2M_W^2}j_{W\mu}j_W^\mu - \frac{\overline{g}_Z^2}{2M_Z^2}j_{Z\mu}j_Z^\mu - \frac{\overline{g}_Z}{M_Z^2}j_{Z\mu}J^\mu - \frac{1}{2M_Z^2}J^\mu J_\mu\,. \tag{C.8}$$

The $\widetilde{X}$ term in J^μ can be dropped using the Bianchi identity

$$\partial_\nu \widetilde{X}^{\mu\nu} = 0\,. \tag{C.9}$$

The equation of motion $\partial_\mu X^{\mu\nu} = j_X^\nu$ can be used to rewrite eq. (C.8) as

$$\mathcal{L} = -\frac{\overline{g}_2^2}{2M_W^2}j_{W\mu}j_W^\mu - \frac{\overline{g}_Z^2}{2M_Z^2}j_{Z\mu}j_Z^\mu + \frac{\overline{g}_Z A_{BW}}{M_Z^2}j_{Z\mu}j_X^\mu - \frac{A_{BW}^2}{2M_Z^2}j_X^\mu j_{X\mu}\,. \tag{C.10}$$

The first two terms give the matching contributions listed in the tables. The last two terms depend on the dark matter currents j_X^μ, which are given in terms of the DM gauge generators, which we have not specified. Their contribution must be added to the matching.

There are also matching contributions from Higgs exchange. However, as discussed in [47], there are additional suppressions to Higgs couplings because, by assumption, the particles in DLEFT all have masses much smaller than the electroweak scale. The Yukawa couplings of the light SM fermions are m_{light}/v, and formally one higher order in the DLEFT power counting. There are similar suppressions of $\phi_a - H$ and $\chi_a - H$ interactions, so that ϕ_a and χ_a remain light after electroweak symmetry breaking. These are:

1. $\phi(H^\dagger H)$ has a $(m_{\text{light}}/v)^3$ suppression.

2. $\phi^2(H^\dagger H)$ has a $(m_{\text{light}}/v)^2$ suppression.

3. $\phi(H^\dagger H)^2$ has a $(m_{\text{light}}/v)^3$ suppression.

4. $\phi^2(H^\dagger H)^2$ has a $(m_{\text{light}}/v)^2$ suppression.

5. $\phi^3(H^\dagger H)$ has a m_{light}/v suppression.

6. $\chi^2(H^\dagger H)$ has a m_{light}/v suppression.

7. $H\overline{\chi}l$ has a m_{light}/v suppression.

8. $H(H^\dagger H)\overline{\chi}l$ has a m_{light}/v suppression.

As a result, Higgs exchange does not contribute at dimension-six, and can be neglected, as was the case in LEFT [47].

DLEFT: dimension 4				$\Delta B = \Delta L = 0$
$(\mathrm{d_{SM}}, \mathrm{d_{DM}})$	Name	Operator	Number	Matching
(2,2)	$\mathcal{O}_{FX}$	$F_{\mu\nu}X_a^{\mu\nu}$	n_X	$\overline{c}\, C_{\underset{a}{BX}} + \frac{v_T^2}{2}\left(\overline{c}\, C_{\underset{a}{H^2BX}} - \overline{s}\, C_{\underset{a}{H^2WX}} \right)$
	$\mathcal{O}_{\widetilde{F}X}$	$\widetilde{F}_{\mu\nu}X_a^{\mu\nu}$	n_X	$\overline{c}\, C_{\underset{a}{\widetilde{B}X}} + \frac{v_T^2}{2}\left(\overline{c}\, C_{\underset{a}{H^2\widetilde{B}X}} - \overline{s}\, C_{\underset{a}{H^2\widetilde{W}X}} \right)$
(3,1)	$\mathcal{O}_{e\phi}$	$(\overline{e}_{L\,p}e_{R\,r})\phi_a$ + h.c.	$n_g^2 n_\phi$ + h.c.	$\frac{v_T}{\sqrt{2}} C_{\underset{pra}{e\phi}}$
	$\mathcal{O}_{u\phi}$	$(\overline{u}_{L\,p}u_{R\,r})\phi_a$ + h.c.	$n_g^2 n_\phi$ + h.c.	$\frac{v_T}{\sqrt{2}} C_{\underset{pra}{u\phi}}$
	$\mathcal{O}_{d\phi}$	$(\overline{d}_{L\,p}d_{R\,r})\phi_a$ + h.c.	$n_g^2 n_\phi$ + h.c.	$\frac{v_T}{\sqrt{2}} C_{\underset{pra}{d\phi}}$

Table 18. Dimension-four $\Delta B = \Delta L = 0$ operators in DLEFT. Note that $\mathcal{O}_{e\phi}$ is not the same as $\mathcal{Q}_{e\phi}$, etc. The first column gives the dimensions of the SM and DM part of the operator, the fourth column is the number of operators, and the fifth column is the additional matching contribution at the EW scale.

DLEFT: dimension 5			$\Delta B = \Delta L = 0$	
$(\mathrm{d_{SM}}, \mathrm{d_{DM}})$	Name	Operator	Number	Matching
(2,3)	$\mathcal{O}_{FX\phi}$	$F_{\mu\nu} X_a^{\mu\nu} \phi_b$	$n_\phi n_X$	$\bar{c}\, C_{\substack{BX\phi\\ab}}$
	$\mathcal{O}_{\widetilde{F}X\phi}$	$\widetilde{F}_{\mu\nu} X_a^{\mu\nu} \phi_b$	$n_\phi n_X$	$\bar{c}\, C_{\substack{\widetilde{B}X\phi\\ab}}$
	$\mathcal{O}_{F\chi}$	$F_{\mu\nu}(\chi_a^T C \sigma^{\mu\nu} \chi_b) + \text{h.c.}$	$\binom{n_\chi}{2} + \text{h.c.}$	$\bar{c}\, C_{\substack{B\chi\\ab}}$
(3,2)	$\mathcal{O}_{e\phi^2}$	$(\bar{e}_{L\,p} e_{R\,r})\phi_a \phi_b + \text{h.c.}$	$n_g^2 \binom{n_\phi+1}{2} + \text{h.c.}$	$\frac{v_T}{\sqrt{2}} C_{\substack{e\phi^2\\prab}}$
	$\mathcal{O}_{u\phi^2}$	$(\bar{u}_{L\,p} u_{R\,r})\phi_a \phi_b + \text{h.c.}$	$n_g^2 \binom{n_\phi+1}{2} + \text{h.c.}$	$\frac{v_T}{\sqrt{2}} C_{\substack{u\phi^2\\prab}}$
	$\mathcal{O}_{d\phi^2}$	$(\bar{d}_{L\,p} d_{R\,r})\phi_a \phi_b + \text{h.c.}$	$n_g^2 \binom{n_\phi+1}{2} + \text{h.c.}$	$\frac{v_T}{\sqrt{2}} C_{\substack{d\phi^2\\prab}}$
	$\mathcal{O}_{eX}$	$(\bar{e}_{L\,p} \sigma_{\mu\nu} e_{R\,r})X_a^{\mu\nu} + \text{h.c.}$	$n_g^2 n_X + \text{h.c.}$	$\frac{v_T}{\sqrt{2}} C_{\substack{eX\\pra}}$
	$\mathcal{O}_{uX}$	$(\bar{u}_{L\,p} \sigma_{\mu\nu} u_{R\,r})X_a^{\mu\nu} + \text{h.c.}$	$n_g^2 n_X + \text{h.c.}$	$\frac{v_T}{\sqrt{2}} C_{\substack{uX\\pra}}$
	$\mathcal{O}_{dX}$	$(\bar{d}_{L\,p} \sigma_{\mu\nu} d_{R\,r})X_a^{\mu\nu} + \text{h.c.}$	$n_g^2 n_X + \text{h.c.}$	$\frac{v_T}{\sqrt{2}} C_{\substack{dX\\pra}}$
(4,1)	$\mathcal{O}_{F\phi}$	$F_{\mu\nu} F^{\mu\nu} \phi_a$	n_ϕ	$\bar{c}^2\, C_{\substack{B\phi\\a}} + \bar{s}^2\, C_{\substack{W\phi\\a}}$
	$\mathcal{O}_{\widetilde{F}\phi}$	$\widetilde{F}_{\mu\nu} F^{\mu\nu} \phi_a$	n_ϕ	$\bar{c}^2\, C_{\substack{\widetilde{B}\phi\\a}} + \bar{s}^2\, C_{\substack{\widetilde{W}\phi\\a}}$
	$\mathcal{O}_{G\phi}$	$G_{\mu\nu}^A G^{A\,\mu\nu} \phi_a$	n_ϕ	$C_{\substack{G\phi\\a}}$
	$\mathcal{O}_{\widetilde{G}\phi}$	$\widetilde{G}_{\mu\nu}^A G^{A\,\mu\nu} \phi_a$	n_ϕ	$C_{\substack{\widetilde{G}\phi\\a}}$

Table 19. Dimension-five $\Delta B = \Delta L = 0$ operators in DLEFT. Note that $\mathcal{O}_{e\phi^2}$ and $\mathcal{O}_{eX}$ are not the same as $\mathcal{Q}_{e\phi^2}$ and $\mathcal{Q}_{eX}$, etc. The first column gives the dimensions of the SM and DM part of the operator, the fourth column is the number of operators, and the fifth column is the additional matching contribution at the EW scale.

DLEFT: dimension 6			$\Delta B = \Delta L = 0$	
$(\mathrm{d_{SM}}, \mathrm{d_{DM}})$	Name	Operator	Number	Matching
(2,4)	$\mathcal{O}_{FX^2}$	$F_\mu{}^\nu X_{a\,\nu}{}^\alpha X_{b\,\alpha}{}^\mu$	$\binom{n_X}{2}$	$\bar{c}\, C_{\substack{BX^2\\ab}}$
	$\mathcal{O}_{\widetilde{F}X^2}$	$\widetilde{F}_\mu{}^\nu X_{a\,\nu}{}^\alpha X_{b\,\alpha}{}^\mu$	$\binom{n_X}{2}$	$\bar{c}\, C_{\substack{\widetilde{B}X^2\\ab}}$
	$\mathcal{O}_{FX\phi^2}$	$F_{\mu\nu} X_a^{\mu\nu} \phi_b \phi_c$	$\binom{n_\phi+1}{2} n_X$	$\bar{c}\, C_{\substack{BX\phi^2\\abc}}$
	$\mathcal{O}_{\widetilde{F}X\phi^2}$	$\widetilde{F}_{\mu\nu} X_a^{\mu\nu} \phi_b \phi_c$	$\binom{n_\phi+1}{2} n_X$	$\bar{c}\, C_{\substack{\widetilde{B}X\phi^2\\abc}}$
	$\mathcal{O}_{F\chi\phi}$	$F_{\mu\nu}(\chi_a^T C \sigma^{\mu\nu} \chi_b)\phi_c + \text{h.c.}$	$n_\phi \binom{n_\chi}{2} + \text{h.c.}$	$\bar{c}\, C_{\substack{B\chi\phi\\abc}}$

Table 20. Dimension-six $\Delta B = \Delta L = 0$ operators in DLEFT, part 1. The first column gives the dimensions of the SM and DM part of the operator, the fourth column is the number of operators, and the fifth column is the additional matching contribution at the EW scale.

DLEFT: dimension 6 $\Delta B = \Delta L = 0$

$(\mathrm{d_{SM}, d_{DM}})$	Name	Operator	Number	Matching
(3,3)	$\mathcal{O}_{e\phi^3}$	$(\bar{e}_{L\,p}e_{R\,r})\phi_a\phi_b\phi_c + \mathrm{h.c.}$	$n_g^2\binom{n_\phi+2}{3} + \mathrm{h.c.}$	0
	$\mathcal{O}_{u\phi^3}$	$(\bar{u}_{L\,p}u_{R\,r})\phi_a\phi_b\phi_c + \mathrm{h.c.}$	$n_g^2\binom{n_\phi+2}{3} + \mathrm{h.c.}$	0
	$\mathcal{O}_{d\phi^3}$	$(\bar{d}_{L\,p}d_{R\,r})\phi_a\phi_b\phi_c + \mathrm{h.c.}$	$n_g^2\binom{n_\phi+2}{3} + \mathrm{h.c.}$	0
	$\mathcal{O}_{\phi\nu}^L$	$(\bar{\nu}_{L\,p}\gamma_\mu\nu_{L\,r})(i\phi_a\overleftrightarrow{\partial^\mu}\phi_b)$	$n_g^2\binom{n_\phi}{2}$	$C_{\underset{prab}{\phi l}} - \frac{\bar{g}_Z^2}{M_Z^2}[Z_\nu]_{pr}[Z_\phi]_{ab}$
	$\mathcal{O}_{\phi e}^L$	$(\bar{e}_{L\,p}\gamma_\mu e_{L\,r})(i\phi_a\overleftrightarrow{\partial^\mu}\phi_b)$	$n_g^2\binom{n_\phi}{2}$	$C_{\underset{prab}{\phi l}} - \frac{\bar{g}_Z^2}{M_Z^2}[Z_{e_L}]_{pr}[Z_\phi]_{ab}$
	$\mathcal{O}_{\phi u}^L$	$(\bar{u}_{L\,p}\gamma_\mu u_{L\,r})(i\phi_a\overleftrightarrow{\partial^\mu}\phi_b)$	$n_g^2\binom{n_\phi}{2}$	$C_{\underset{prab}{\phi q}} - \frac{\bar{g}_Z^2}{M_Z^2}[Z_{u_L}]_{pr}[Z_\phi]_{ab}$
	$\mathcal{O}_{\phi d}^L$	$(\bar{d}_{L\,p}\gamma_\mu d_{L\,r})(i\phi_a\overleftrightarrow{\partial^\mu}\phi_b)$	$n_g^2\binom{n_\phi}{2}$	$C_{\underset{prab}{\phi q}} - \frac{\bar{g}_Z^2}{M_Z^2}[Z_{d_L}]_{pr}[Z_\phi]_{ab}$
	$\mathcal{O}_{\phi e}^R$	$(\bar{e}_{R\,p}\gamma_\mu e_{R\,r})(i\phi_a\overleftrightarrow{\partial^\mu}\phi_b)$	$n_g^2\binom{n_\phi}{2}$	$C_{\underset{prab}{\phi e}} - \frac{\bar{g}_Z^2}{M_Z^2}[Z_{e_R}]_{pr}[Z_\phi]_{ab}$
	$\mathcal{O}_{\phi u}^R$	$(\bar{u}_{R\,p}\gamma_\mu u_{R\,r})(i\phi_a\overleftrightarrow{\partial^\mu}\phi_b)$	$n_g^2\binom{n_\phi}{2}$	$C_{\underset{prab}{\phi u}} - \frac{\bar{g}_Z^2}{M_Z^2}[Z_{u_R}]_{pr}[Z_\phi]_{ab}$
	$\mathcal{O}_{\phi d}^R$	$(\bar{d}_{R\,p}\gamma_\mu d_{R\,r})(i\phi_a\overleftrightarrow{\partial^\mu}\phi_b)$	$n_g^2\binom{n_\phi}{2}$	$C_{\underset{prab}{\phi d}} - \frac{\bar{g}_Z^2}{M_Z^2}[Z_{d_R}]_{pr}[Z_\phi]_{ab}$
	$\mathcal{O}_{eX\phi}$	$(\bar{e}_{L\,p}\sigma_{\mu\nu}e_{R\,r})X_a^{\mu\nu}\phi_b + \mathrm{h.c.}$	$n_g^2 n_\phi n_X + \mathrm{h.c.}$	0
	$\mathcal{O}_{uX\phi}$	$(\bar{u}_{L\,p}\sigma_{\mu\nu}u_{R\,r})X_a^{\mu\nu}\phi_b + \mathrm{h.c.}$	$n_g^2 n_\phi n_X + \mathrm{h.c.}$	0
	$\mathcal{O}_{dX\phi}$	$(\bar{d}_{L\,p}\sigma_{\mu\nu}d_{R\,r})X_a^{\mu\nu}\phi_b + \mathrm{h.c.}$	$n_g^2 n_\phi n_X + \mathrm{h.c.}$	0

Table 21. Dimension-six $\Delta B = \Delta L = 0$ operators in DLEFT, part 2. The first column gives the dimensions of the SM and DM part of the operator, the fourth column is the number of operators, and the fifth column is the additional matching contribution at the EW scale.

DLEFT: dimension 6			$\Delta B = \Delta L = 0$	
$(\mathrm{d_{SM}}, \mathrm{d_{DM}})$	Name	Operator	Number	Matching
(3,3)	$\mathcal{O}_{\nu\chi}^{V,LR}$	$(\overline{\nu}_{L\,p}\gamma_\mu \nu_{L\,r})(\overline{\chi}_a \gamma^\mu \chi_b)$	$n_g^2 n_\chi^2$	$\underset{prab}{C_{l\chi}} - \frac{\overline{g}_Z^2}{M_Z^2}[Z_\nu]_{pr}[Z_\chi]_{ab}$
	$\mathcal{O}_{e\chi}^{V,LR}$	$(\overline{e}_{L\,p}\gamma_\mu e_{L\,r})(\overline{\chi}_a \gamma^\mu \chi_b)$	$n_g^2 n_\chi^2$	$\underset{prab}{C_{l\chi}} - \frac{\overline{g}_Z^2}{M_Z^2}[Z_{e_L}]_{pr}[Z_\chi]_{ab}$
	$\mathcal{O}_{u\chi}^{V,LR}$	$(\overline{u}_{L\,p}\gamma_\mu u_{L\,r})(\overline{\chi}_a \gamma^\mu \chi_b)$	$n_g^2 n_\chi^2$	$\underset{prab}{C_{q\chi}} - \frac{\overline{g}_Z^2}{M_Z^2}[Z_{u_L}]_{pr}[Z_\chi]_{ab}$
	$\mathcal{O}_{d\chi}^{V,LR}$	$(\overline{d}_{L\,p}\gamma_\mu d_{L\,r})(\overline{\chi}_a \gamma^\mu \chi_b)$	$n_g^2 n_\chi^2$	$\underset{prab}{C_{q\chi}} - \frac{\overline{g}_Z^2}{M_Z^2}[Z_{d_L}]_{pr}[Z_\chi]_{ab}$
	$\mathcal{O}_{e\chi}^{V,RR}$	$(\overline{e}_{R\,p}\gamma_\mu e_{R\,r})(\overline{\chi}_a \gamma^\mu \chi_b)$	$n_g^2 n_\chi^2$	$\underset{prab}{C_{e\chi}} - \frac{\overline{g}_Z^2}{M_Z^2}[Z_{e_R}]_{pr}[Z_\chi]_{ab}$
	$\mathcal{O}_{u\chi}^{V,RR}$	$(\overline{u}_{R\,p}\gamma_\mu u_{R\,r})(\overline{\chi}_a \gamma^\mu \chi_b)$	$n_g^2 n_\chi^2$	$\underset{prab}{C_{u\chi}} - \frac{\overline{g}_Z^2}{M_Z^2}[Z_{u_R}]_{pr}[Z_\chi]_{ab}$
	$\mathcal{O}_{d\chi}^{V,RR}$	$(\overline{d}_{R\,p}\gamma_\mu d_{R\,r})(\overline{\chi}_a \gamma^\mu \chi_b)$	$n_g^2 n_\chi^2$	$\underset{prab}{C_{d\chi}} - \frac{\overline{g}_Z^2}{M_Z^2}[Z_{d_R}]_{pr}[Z_\chi]_{ab}$
	$\mathcal{O}_{e\chi}^{S,RR}$	$(\overline{e}_{L\,p} e_{R\,r})(\chi_a^T C \chi_b) + \mathrm{h.c.}$	$n_g^2 \binom{n_\chi+1}{2} + \mathrm{h.c.}$	0
	$\mathcal{O}_{u\chi}^{S,RR}$	$(\overline{u}_{L\,p} u_{R\,r})(\chi_a^T C \chi_b) + \mathrm{h.c.}$	$n_g^2 \binom{n_\chi+1}{2} + \mathrm{h.c.}$	0
	$\mathcal{O}_{d\chi}^{S,RR}$	$(\overline{d}_{L\,p} d_{R\,r})(\chi_a^T C \chi_b) + \mathrm{h.c.}$	$n_g^2 \binom{n_\chi+1}{2} + \mathrm{h.c.}$	0
	$\mathcal{O}_{e\chi}^{T,RR}$	$(\overline{e}_{L\,p} \sigma^{\mu\nu} e_{R\,r})(\chi_a^T C \sigma_{\mu\nu} \chi_b) + \mathrm{h.c.}$	$n_g^2 \binom{n_\chi}{2} + \mathrm{h.c.}$	0
	$\mathcal{O}_{u\chi}^{T,RR}$	$(\overline{u}_{L\,p} \sigma^{\mu\nu} u_{R\,r})(\chi_a^T C \sigma_{\mu\nu} \chi_b) + \mathrm{h.c.}$	$n_g^2 \binom{n_\chi}{2} + \mathrm{h.c.}$	0
	$\mathcal{O}_{d\chi}^{T,RR}$	$(\overline{d}_{L\,p} \sigma^{\mu\nu} d_{R\,r})(\chi_a^T C \sigma_{\mu\nu} \chi_b) + \mathrm{h.c.}$	$n_g^2 \binom{n_\chi}{2} + \mathrm{h.c.}$	0
	$\mathcal{O}_{e\chi}^{S,LR}$	$(\overline{e}_{R\,p} e_{L\,r})(\chi_a^T C \chi_b) + \mathrm{h.c.}$	$n_g^2 \binom{n_\chi+1}{2} + \mathrm{h.c.}$	0
	$\mathcal{O}_{u\chi}^{S,LR}$	$(\overline{u}_{R\,p} u_{L\,r})(\chi_a^T C \chi_b) + \mathrm{h.c.}$	$n_g^2 \binom{n_\chi+1}{2} + \mathrm{h.c.}$	0
	$\mathcal{O}_{d\chi}^{S,LR}$	$(\overline{d}_{R\,p} d_{L\,r})(\chi_a^T C \chi_b) + \mathrm{h.c.}$	$n_g^2 \binom{n_\chi+1}{2} + \mathrm{h.c.}$	0

Table 22. Dimension-six $\Delta B = \Delta L = 0$ operators in DLEFT, part 3. The first column gives the dimensions of the SM and DM part of the operator, the fourth column is the number of operators, and the fifth column is the additional matching contribution at the EW scale.

DLEFT: dimension 6			$\Delta B = \Delta L = 0$	
$(\mathrm{d_{SM}}, \mathrm{d_{DM}})$	Name	Operator	Number	Matching
(4,2)	$\mathcal{O}_{F\phi^2}$	$F_{\mu\nu} F^{\mu\nu} \phi_a \phi_b$	$\binom{n_\phi+1}{2}$	$\overline{c}^2 \underset{ab}{C_{B\phi^2}} + \overline{s}^2 \underset{ab}{C_{W\phi^2}}$
	$\mathcal{O}_{\widetilde{F}\phi^2}$	$\widetilde{F}_{\mu\nu} F^{\mu\nu} \phi_a \phi_b$	$\binom{n_\phi+1}{2}$	$\overline{c}^2 \underset{ab}{C_{\widetilde{B}\phi^2}} + \overline{s}^2 \underset{ab}{C_{\widetilde{W}\phi^2}}$
	$\mathcal{O}_{G\phi^2}$	$G_{\mu\nu}^A G^{A\,\mu\nu} \phi_a \phi_b$	$\binom{n_\phi+1}{2}$	$\underset{ab}{C_{G\phi^2}}$
	$\mathcal{O}_{\widetilde{G}\phi^2}$	$\widetilde{G}_{\mu\nu}^A G^{A\,\mu\nu} \phi_a \phi_b$	$\binom{n_\phi+1}{2}$	$\underset{ab}{C_{\widetilde{G}\phi^2}}$
(5,1)	$\mathcal{O}_{eF\phi}$	$(\overline{e}_{L\,p} \sigma^{\mu\nu} e_{R\,r}) F_{\mu\nu} \phi_a + \mathrm{h.c.}$	$n_g^2 n_\phi + \mathrm{h.c.}$	0
	$\mathcal{O}_{uF\phi}$	$(\overline{u}_{L\,p} \sigma^{\mu\nu} u_{R\,r}) F_{\mu\nu} \phi_a + \mathrm{h.c.}$	$n_g^2 n_\phi + \mathrm{h.c.}$	0
	$\mathcal{O}_{dF\phi}$	$(\overline{d}_{L\,p} \sigma^{\mu\nu} d_{R\,r}) F_{\mu\nu} \phi_a + \mathrm{h.c.}$	$n_g^2 n_\phi + \mathrm{h.c.}$	0
	$\mathcal{O}_{uG\phi}$	$(\overline{u}_{L\,p} \sigma^{\mu\nu} T^A u_{R\,r}) G_{\mu\nu}^A \phi_a + \mathrm{h.c.}$	$n_g^2 n_\phi + \mathrm{h.c.}$	0
	$\mathcal{O}_{dG\phi}$	$(\overline{d}_{L\,p} \sigma^{\mu\nu} T^A d_{R\,r}) G_{\mu\nu}^A \phi_a + \mathrm{h.c.}$	$n_g^2 n_\phi + \mathrm{h.c.}$	0

Table 23. Dimension-six $\Delta B = \Delta L = 0$ operators in DLEFT, part 4. The first column gives the dimensions of the SM and DM part of the operator, the fourth column is the number of operators, and the fifth column is the additional matching contribution at the EW scale.

DLEFT: dimension 3 $\mathbf{\Delta B = 0,\ \Delta L = 1}$ + h.c.

$(\mathrm{d_{SM}, d_{DM}})$	Name	Operator	Number	Matching
$(3/2, 3/2)$	$\mathcal{O}_{\chi\nu}$	$(\overline{\chi}_a\nu_{L\,p})$	$n_g n_\chi$	$-\frac{v_T}{\sqrt{2}} C_{\substack{H\chi l \\ ap}} - \frac{v_T^3}{2\sqrt{2}} C_{\substack{H^3\chi l \\ ap}}$

Table 24. Dimension-three $\Delta B = 0$, $\Delta L = 1$ operator in DLEFT. The first column gives the dimensions of the SM and DM part of the operator, the fourth column is the number of operators, and the fifth column is the additional matching contribution at the EW scale.

DLEFT: dimension 4 $\mathbf{\Delta B = 0,\ \Delta L = 1}$ + h.c.

$(\mathrm{d_{SM}, d_{DM}})$	Name	Operator	Number	Matching
$(3/2, 5/2)$	$\mathcal{O}_{\chi\nu\phi}$	$(\overline{\chi}_a\nu_{L\,p})\phi_b$	$n_g n_\phi n_\chi$	$-\frac{v_T}{\sqrt{2}} C_{\substack{H\chi l\phi \\ apb}}$

Table 25. Dimension-four $\Delta B = 0$, $\Delta L = 1$ operator in DLEFT. The first column gives the dimensions of the SM and DM part of the operator, the fourth column is the number of operators, and the fifth column is the additional matching contribution at the EW scale.

DLEFT: dimension 5 $\mathbf{\Delta B = 0,\ \Delta L = 1}$ + h.c.

$(\mathrm{d_{SM}, d_{DM}})$	Name	Operator	Number	Matching
$(3/2, 7/2)$	$\mathcal{O}_{\chi\nu\phi^2}$	$(\overline{\chi}_a\nu_{L\,p})\phi_b\phi_c$	$n_g\binom{n_\phi+1}{2}n_\chi$	$-\frac{v_T}{\sqrt{2}} C_{\substack{H\chi l\phi^2 \\ apbc}}$
	$\mathcal{O}_{\chi\nu X}$	$(\overline{\chi}_a\sigma^{\mu\nu}\nu_{L\,p})X_{b\,\mu\nu}$	$n_g n_\chi n_X$	$-\frac{v_T}{\sqrt{2}} C_{\substack{H\chi l X \\ apb}}$
$(7/2, 3/2)$	$\mathcal{O}_{F\chi\nu}$	$F_{\mu\nu}(\overline{\chi}_a\sigma^{\mu\nu}\nu_{L\,p})$	$n_g n_\chi$	$\frac{v_T}{\sqrt{2}}\left(\overline{c}\, C_{\substack{HB\chi l \\ ap}} - \overline{s}\, C_{\substack{HW\chi l \\ ap}}\right)$

Table 26. Dimension-five $\Delta B = 0$, $\Delta L = 1$ operators in DLEFT. The first column gives the dimensions of the SM and DM part of the operator, the fourth column is the number of operators, and the fifth column is the additional matching contribution at the EW scale.

DLEFT: dimension 6 $\mathbf{\Delta B = 0,\ \Delta L = 1}$ + h.c.

$(\mathrm{d_{SM}, d_{DM}})$	Name	Operator	Number	Matching
$(3/2,\ 9/2)$	$\mathcal{O}_{\chi\nu\phi^3}$	$(\overline{\chi}_a\nu_{L\,p})\phi_b\phi_c\phi_d$	$n_g\binom{n_\phi+2}{3}n_\chi$	0
	$\mathcal{O}_{\chi\nu X\phi}$	$(\overline{\chi}_a\sigma^{\mu\nu}\nu_{L\,p})X_{b\,\mu\nu}\phi_c$	$n_g n_\phi n_\chi n_X$	0
	$\mathcal{O}_{\phi\chi\nu}^{L}$	$(\chi_a^T C\gamma_\mu \nu_{L\,p})(i\phi_b\overleftrightarrow{\partial}^\mu\phi_c)$	$n_g\binom{n_\phi}{2}n_\chi$	0
	$\mathcal{O}_{\chi\nu\chi}^{S,LR}$	$(\overline{\chi}_a\nu_{L\,p})(\chi_b^T C\chi_c)$	$n_g n_\chi\binom{n_\chi+1}{2}$	0
	$\mathcal{O}_{\chi\nu\overline{\chi}}^{S,LL}$	$(\overline{\chi}_a\nu_{L\,p})(\overline{\chi}_b C\overline{\chi}_c^T)$	$\frac{1}{3}n_g n_\chi(n_\chi^2-1)$	0
$(7/2,\ 5/2)$	$\mathcal{O}_{F\chi\nu\phi}$	$F_{\mu\nu}(\overline{\chi}_a\sigma^{\mu\nu}\nu_{L\,p})\phi_b$	$n_g n_\phi n_\chi$	0
$(9/2,\ 3/2)$	$\mathcal{O}_{\nu\chi\nu}^{V,LL}$	$(\overline{\nu}_{L\,p}\gamma^\mu\nu_{L\,r})(\chi_a^T C\gamma_\mu\nu_{L\,s})$	$n_g\binom{n_g+1}{2}n_\chi$	0
	$\mathcal{O}_{e\chi\nu}^{V,LL}$	$(\overline{e}_{L\,p}\gamma^\mu e_{L\,r})(\chi_a^T C\gamma_\mu\nu_{L\,s})$	$n_g^3 n_\chi$	0
	$\mathcal{O}_{u\chi\nu}^{V,LL}$	$(\overline{u}_{L\,p}\gamma^\mu u_{L\,r})(\chi_a^T C\gamma_\mu\nu_{L\,s})$	$n_g^3 n_\chi$	0
	$\mathcal{O}_{d\chi\nu}^{V,LL}$	$(\overline{d}_{L\,p}\gamma^\mu d_{L\,r})(\chi_a^T C\gamma_\mu\nu_{L\,s})$	$n_g^3 n_\chi$	0
	$\mathcal{O}_{du\chi e}^{V,LL}$	$(\overline{d}_{L\,p}\gamma_\mu u_{L\,r})(\chi_a^T C\gamma^\mu e_{L\,s})$	$n_g^3 n_\chi$	0

Table 27. Dimension-six $\Delta B = 0$, $\Delta L = 1$ operators in DLEFT, part 1. The first column gives the dimensions of the SM and DM part of the operator, the fourth column is the number of operators, and the fifth column is the additional matching contribution at the EW scale.

DLEFT: dimension 6 $\qquad\qquad$ $\boldsymbol{\Delta B = 0,\ \Delta L = 1}$ + h.c.

$(\mathrm{d_{SM}}, \mathrm{d_{DM}})$	Name	Operator	Number	Matching
(9/2,3/2)	$\mathcal{O}_{e\chi\nu}^{V,RL}$	$(\bar{e}_{Rp}\gamma^\mu e_{Rr})(\chi_a^T C\gamma_\mu \nu_{Ls})$	$n_g^3 n_\chi$	0
	$\mathcal{O}_{u\chi\nu}^{V,RL}$	$(\bar{u}_{Rp}\gamma^\mu u_{Rr})(\chi_a^T C\gamma_\mu \nu_{Ls})$	$n_g^3 n_\chi$	0
	$\mathcal{O}_{d\chi\nu}^{V,RL}$	$(\bar{d}_{Rp}\gamma^\mu d_{Rr})(\chi_a^T C\gamma_\mu \nu_{Ls})$	$n_g^3 n_\chi$	0
	$\mathcal{O}_{du\chi e}^{V,RL}$	$(\bar{d}_{Rp}\gamma_\mu u_{Rr})(\chi_a^T C\gamma^\mu e_{Ls})$	$n_g^3 n_\chi$	0
	$\mathcal{O}_{du\chi e}^{V,LR}$	$(\bar{d}_{Lp}\gamma^\mu u_{Lr})(\bar{\chi}_a\gamma_\mu e_{Rs})$	$n_g^3 n_\chi$	$-\frac{\bar{g}_2^2}{2M_W^2}[W_q]_{rp}^*[W_\chi]_{as}$
	$\mathcal{O}_{du\chi e}^{V,RR}$	$(\bar{d}_{Rp}\gamma_\mu u_{Rr})(\bar{\chi}_a\gamma^\mu e_{Rs})$	$n_g^3 n_\chi$	$C_{\substack{du\chi e \\ pras}} - \frac{\bar{g}_2^2}{2M_W^2}[W_R]_{rp}^*[W_\chi]_{as}$
	$\mathcal{O}_{du\chi e}^{S,RR}$	$(\bar{d}_{Lp} u_{Rr})(\chi_a^T C e_{Rs})$	$n_g^3 n_\chi$	0
	$\mathcal{O}_{du\chi e}^{T,RR}$	$(\bar{d}_{Lp}\sigma_{\mu\nu} u_{Rr})(\chi_a^T C\sigma^{\mu\nu} e_{Rs})$	$n_g^3 n_\chi$	0
	$\mathcal{O}_{e\chi\nu}^{S,RL}$	$(\bar{e}_{Lp} e_{Rr})(\bar{\chi}_a \nu_{Ls})$	$n_g^3 n_\chi$	$\frac{\bar{g}_2^2}{M_W^2}[W_l]_{sp}^*[W_\chi]_{ar}$
	$\mathcal{O}_{u\chi\nu}^{S,RL}$	$(\bar{u}_{Lp} u_{Rr})(\bar{\chi}_a \nu_{Ls})$	$n_g^3 n_\chi$	$C_{\substack{qu\chi l \\ pras}}$
	$\mathcal{O}_{d\chi\nu}^{S,RL}$	$(\bar{d}_{Lp} d_{Rr})(\bar{\chi}_a \nu_{Ls})$	$n_g^3 n_\chi$	0
	$\mathcal{O}_{du\chi e}^{S,RL}$	$(\bar{d}_{Lp} u_{Rr})(\bar{\chi}_a e_{Ls})$	$n_g^3 n_\chi$	$C_{\substack{qu\chi l \\ pras}}$
	$\mathcal{O}_{e\chi\nu}^{S,LL}$	$(\bar{e}_{Rp} e_{Lr})(\bar{\chi}_a \nu_{Ls})$	$n_g^3 n_\chi$	$-\frac{1}{2}C_{\substack{le\chi \\ srpa}}^{(1)} + \frac{1}{2}C_{\substack{le\chi \\ rspa}}^{(1)} - 6C_{\substack{le\chi \\ srpa}}^{(3)} - 6C_{\substack{le\chi \\ rspa}}^{(3)}$
	$\mathcal{O}_{u\chi\nu}^{S,LL}$	$(\bar{u}_{Rp} u_{Lr})(\bar{\chi}_a \nu_{Ls})$	$n_g^3 n_\chi$	0
	$\mathcal{O}_{d\chi\nu}^{S,LL}$	$(\bar{d}_{Rp} d_{Lr})(\bar{\chi}_a \nu_{Ls})$	$n_g^3 n_\chi$	$-C_{\substack{dq\chi l \\ pras}}^{(1)}$
	$\mathcal{O}_{du\chi e}^{S,LL}$	$(\bar{d}_{Rp} u_{Lr})(\bar{\chi}_a e_{Ls})$	$n_g^3 n_\chi$	$C_{\substack{dq\chi l \\ pras}}^{(1)}$
	$\mathcal{O}_{e\chi\nu}^{T,LL}$	$(\bar{e}_{Rp}\sigma^{\mu\nu} e_{Lr})(\bar{\chi}_a \sigma^{\mu\nu} \nu_{Ls})$	$n_g^3 n_\chi$	$\frac{1}{8}C_{\substack{le\chi \\ srpa}}^{(1)} - \frac{1}{8}C_{\substack{le\chi \\ rspa}}^{(1)} - \frac{1}{2}C_{\substack{le\chi \\ srpa}}^{(3)} - \frac{1}{2}C_{\substack{le\chi \\ rspa}}^{(3)}$
	$\mathcal{O}_{u\chi\nu}^{T,LL}$	$(\bar{u}_{Rp}\sigma^{\mu\nu} u_{Lr})(\bar{\chi}_a \sigma^{\mu\nu} \nu_{Ls})$	$n_g^3 n_\chi$	0
	$\mathcal{O}_{d\chi\nu}^{T,LL}$	$(\bar{d}_{Rp}\sigma^{\mu\nu} d_{Lr})(\bar{\chi}_a \sigma^{\mu\nu} \nu_{Ls})$	$n_g^3 n_\chi$	$-C_{\substack{dq\chi l \\ pras}}^{(3)}$
	$\mathcal{O}_{du\chi e}^{T,LL}$	$(\bar{d}_{Rp}\sigma_{\mu\nu} u_{Lr})(\bar{\chi}_a \sigma^{\mu\nu} e_{Ls})$	$n_g^3 n_\chi$	$C_{\substack{dq\chi l \\ pras}}^{(3)}$
	$\mathcal{O}_{du\chi e}^{S,LR}$	$(\bar{d}_{Rp} u_{Lr})(\chi_a^T C e_{Rs})$	$n_g^3 n_\chi$	0

Table 28. Dimension-six $\Delta B = 0$, $\Delta L = 1$ operators in DLEFT, part 2. The first column gives the dimensions of the SM and DM part of the operator, the fourth column is the number of operators, and the fifth column is the additional matching contribution at the EW scale.

DLEFT: dimension 4 $\qquad$ $\boldsymbol{\Delta B = 0,\ \Delta L = 2}$ + h.c.

$(\mathrm{d_{SM}}, \mathrm{d_{DM}})$	Name	Operator	Number	Matching
(3,1)	$\mathcal{O}_{\nu\phi}$	$(\nu_{Lp}^T C\nu_{Lr})\phi_a$	$\binom{n_g+1}{2}n_\phi$	$\frac{v_T^2}{2}C_{\substack{\nu\nu\phi \\ pra}}$

Table 29. Dimension-four $\Delta B = 0$, $\Delta L = 2$ operator in DLEFT. The first column gives the dimensions of the SM and DM part of the operator, the fourth column is the number of operators, and the fifth column is the additional matching contribution at the EW scale.

DLEFT: dimension 5		$\Delta B = 0$, $\Delta L = 2 +$ h.c.		
$(\mathrm{d_{SM}}, \mathrm{d_{DM}})$	Name	Operator	Number	Matching
(3,2)	$\mathcal{O}_{\nu\phi^2}$	$(\nu_{L\,p}^T C\nu_{L\,r})\phi_a\phi_b$	$\binom{n_g+1}{2}\binom{n_\phi+1}{2}$	0
	$\mathcal{O}_{\nu X}$	$(\nu_{L\,p}^T C\sigma_{\mu\nu}\nu_{L\,r})X_a^{\mu\nu}$	$\binom{n_\chi}{2}n_X$	0

Table 30. Dimension-five $\Delta B = 0$, $\Delta L = 2$ operators in DLEFT. The first column gives the dimensions of the SM and DM part of the operator, the fourth column is the number of operators, and the fifth column is the additional matching contribution at the EW scale.

DLEFT: dimension 6		$\Delta B = 0$, $\Delta L = 2 +$ h.c.		
$(\mathrm{d_{SM}}, \mathrm{d_{DM}})$	Name	Operator	Number	Matching
(3,3)	$\mathcal{O}_{\nu\phi^3}$	$(\nu_{L\,p}^T C\nu_{L\,r})\phi_a\phi_b\phi_c$	$\binom{n_g+1}{2}\binom{n_\phi+2}{3}$	0
	$\mathcal{O}_{\nu X\phi}$	$(\nu_{L\,p}^T C\sigma_{\mu\nu}\nu_{L\,r})X_a^{\mu\nu}\phi_b$	$\binom{n_g}{2}n_\phi n_X$	0
	$\mathcal{O}_{\nu\bar\chi}^{S,LL}$	$(\nu_{L\,p}^T C\nu_{L\,r})(\bar\chi_a C\bar\chi_b^T)$	$\binom{n_g+1}{2}\binom{n_\chi+1}{2}$	0
	$\mathcal{O}_{\nu\bar\chi}^{T,LL}$	$(\nu_{L\,p}^T C\sigma_{\mu\nu}\nu_{L\,r})(\bar\chi_a\sigma^{\mu\nu}C\bar\chi_b^T)$	$\binom{n_g}{2}\binom{n_\chi}{2}$	0
	$\mathcal{O}_{\nu\chi}^{S,LR}$	$(\nu_{L\,p}^T C\nu_{L\,r})(\chi_a^T C\chi_b)$	$\binom{n_g+1}{2}\binom{n_\chi+1}{2}$	0
(5,1)	$\mathcal{O}_{\nu F\phi}$	$(\nu_{L\,p}^T C\sigma^{\mu\nu}\nu_{L\,r})F_{\mu\nu}\phi_a$	$\binom{n_g}{2}n_\phi$	0

Table 31. Dimension-six $\Delta B = 0$, $\Delta L = 2$ operators in DLEFT. The first column gives the dimensions of the SM and DM part of the operator, the fourth column is the number of operators, and the fifth column is the additional matching contribution at the EW scale.

DLEFT: dimension 6		$\Delta B = 0$, $\Delta L = 3 +$ h.c.		
$(\mathrm{d_{SM}}, \mathrm{d_{DM}})$	Name	Operator	Number	Matching
(9/2,5/2)	$\mathcal{O}_{\nu\chi\nu}^{S,LL}$	$(\nu_{L\,p}^T C\nu_{L\,r})(\bar\chi_a\nu_{L\,s})$	$\frac{1}{3}n_g(n_g^2-1)n_\chi$	0

Table 32. Dimension-six $\Delta B = 0$, $\Delta L = 3$ operator in DLEFT. The first column gives the dimensions of the SM and DM part of the operator, the fourth column is the number of operators, and the fifth column is the additional matching contribution at the EW scale.

DLEFT: dimension 6		$\Delta L = 0,\ \Delta B = 1 +$ h.c.		
$(\mathrm{d}_{\mathrm{SM}}, \mathrm{d}_{\mathrm{DM}})$	Name	Operator	Number	Matching
(9/2,3/2)	$\mathcal{O}^{S,LR}_{udd}$	$\epsilon^{\alpha\beta\gamma}(u^{\alpha\,T}_{L\,p}Cd^{\beta}_{L\,r})(\chi^T_a Cd^{\gamma}_{R\,s})$	$n_g^3 n_\chi$	$C_{\substack{qqd\\pras}} + C_{\substack{qqd\\rpas}}$
	$\mathcal{O}^{S,LL}_{ddu}$	$\epsilon^{\alpha\beta\gamma}(d^{\alpha\,T}_{L\,p}Cd^{\beta}_{L\,r})(\overline{\chi}_a u^{\gamma}_{L\,s})$	$n_g\binom{n_g}{2}n_\chi$	0
	$\mathcal{O}^{T,LL}_{ddu}$	$\epsilon^{\alpha\beta\gamma}(d^{\alpha\,T}_{L\,p}C\sigma_{\mu\nu}d^{\beta}_{L\,r})(\overline{\chi}_a \sigma^{\mu\nu}u^{\gamma}_{L\,s})$	$n_g\binom{n_g+1}{2}n_\chi$	0
	$\mathcal{O}^{S,RL}_{ddu}$	$\epsilon^{\alpha\beta\gamma}(d^{\alpha\,T}_{R\,p}Cd^{\beta}_{R\,r})(\overline{\chi}_a u^{\gamma}_{L\,s})$	$n_g\binom{n_g}{2}n_\chi$	0
	$\mathcal{O}^{S,RL}_{dud}$	$\epsilon^{\alpha\beta\gamma}(d^{\alpha\,T}_{R\,p}Cu^{\beta}_{R\,r})(\overline{\chi}_a d^{\gamma}_{L\,s})$	$n_g^3 n_\chi$	0
	$\mathcal{O}^{S,LR}_{ddu}$	$\epsilon^{\alpha\beta\gamma}(d^{\alpha\,T}_{L\,p}Cd^{\beta}_{L\,r})(\chi^T_a Cu^{\gamma}_{R\,s})$	$n_g\binom{n_g}{2}n_\chi$	0
	$\mathcal{O}^{S,RR}_{ddu}$	$\epsilon^{\alpha\beta\gamma}(d^{\alpha\,T}_{R\,p}Cd^{\beta}_{R\,r})(\chi^T_a Cu^{\gamma}_{R\,s})$	$n_g\binom{n_g}{2}n_\chi$	$C^{(1)}_{\substack{ddu\\pras}}$
	$\mathcal{O}^{T,RR}_{ddu}$	$\epsilon^{\alpha\beta\gamma}(d^{\alpha\,T}_{R\,p}C\sigma^{\mu\nu}d^{\beta}_{R\,r})(\chi^T_a C\sigma_{\mu\nu}u^{\gamma}_{R\,s})$	$n_g\binom{n_g+1}{2}n_\chi$	$C^{(3)}_{\substack{ddu\\pras}}$

Table 33. Dimension-six $\Delta L = 0$, $\Delta B = 1$ operators in DLEFT. The first column gives the dimensions of the SM and DM part of the operator, the fourth column is the number of operators, and the fifth column is the additional matching contribution at the EW scale.

References

[1] J. Fan, M. Reece and L.-T. Wang, *Non-relativistic effective theory of dark matter direct detection*, *JCAP* **11** (2010) 042 [arXiv:1008.1591] [INSPIRE].

[2] A.L. Fitzpatrick, W. Haxton, E. Katz, N. Lubbers and Y. Xu, *Model Independent Direct Detection Analyses*, arXiv:1211.2818 [INSPIRE].

[3] A.L. Fitzpatrick, W. Haxton, E. Katz, N. Lubbers and Y. Xu, *The Effective Field Theory of Dark Matter Direct Detection*, *JCAP* **02** (2013) 004 [arXiv:1203.3542] [INSPIRE].

[4] B. Bellazzini, M. Cliche and P. Tanedo, *Effective theory of self-interacting dark matter*, *Phys. Rev. D* **88** (2013) 083506 [arXiv:1307.1129] [INSPIRE].

[5] M. Cirelli, E. Del Nobile and P. Panci, *Tools for model-independent bounds in direct dark matter searches*, *JCAP* **10** (2013) 019 [arXiv:1307.5955] [INSPIRE].

[6] R. Catena and P. Gondolo, *Global fits of the dark matter-nucleon effective interactions*, *JCAP* **09** (2014) 045 [arXiv:1405.2637] [INSPIRE].

[7] G. Ovanesyan, T.R. Slatyer and I.W. Stewart, *Heavy Dark Matter Annihilation from Effective Field Theory*, *Phys. Rev. Lett.* **114** (2015) 211302 [arXiv:1409.8294] [INSPIRE].

[8] SuperCDMS collaboration, *Dark matter effective field theory scattering in direct detection experiments*, *Phys. Rev. D* **91** (2015) 092004 [arXiv:1503.03379] [INSPIRE].

[9] R. Catena, K. Fridell and M.B. Krauss, *Non-relativistic Effective Interactions of Spin 1 Dark Matter*, *JHEP* **08** (2019) 030 [arXiv:1907.02910] [INSPIRE].

[10] E. Del Nobile, *The Theory of Direct Dark Matter Detection: A Guide to Computations*, arXiv:2104.12785 [INSPIRE].

[11] M. Hoferichter, P. Klos and A. Schwenk, *Chiral power counting of one- and two-body currents in direct detection of dark matter*, *Phys. Lett. B* **746** (2015) 410 [arXiv:1503.04811] [INSPIRE].

[12] M. Hoferichter, P. Klos, J. Menéndez and A. Schwenk, *Analysis strategies for general spin-independent WIMP-nucleus scattering*, *Phys. Rev. D* **94** (2016) 063505 [arXiv:1605.08043] [INSPIRE].

[13] M. Hoferichter, P. Klos, J. Menéndez and A. Schwenk, *Nuclear structure factors for general spin-independent WIMP-nucleus scattering*, *Phys. Rev. D* **99** (2019) 055031 [arXiv:1812.05617] [INSPIRE].

[14] A. De Simone and T. Jacques, *Simplified models vs. effective field theory approaches in dark matter searches*, *Eur. Phys. J. C* **76** (2016) 367 [arXiv:1603.08002] [INSPIRE].

[15] R. Harnik and G.D. Kribs, *An Effective Theory of Dirac Dark Matter*, *Phys. Rev. D* **79** (2009) 095007 [arXiv:0810.5557] [INSPIRE].

[16] J. Kopp, T. Schwetz and J. Zupan, *Global interpretation of direct Dark Matter searches after CDMS-II results*, *JCAP* **02** (2010) 014 [arXiv:0912.4264] [INSPIRE].

[17] J. Goodman, M. Ibe, A. Rajaraman, W. Shepherd, T.M.P. Tait and H.-B. Yu, *Gamma Ray Line Constraints on Effective Theories of Dark Matter*, *Nucl. Phys. B* **844** (2011) 55 [arXiv:1009.0008] [INSPIRE].

[18] B. Barman, D. Borah and R. Roshan, *Effective Theory of Freeze-in Dark Matter*, *JCAP* **11** (2020) 021 [arXiv:2007.08768] [INSPIRE].

[19] B. Barman, S. Bhattacharya and B. Grzadkowski, *Feebly coupled vector boson dark matter in effective theory*, *JHEP* **12** (2020) 162 [arXiv:2009.07438] [INSPIRE].

[20] K. Cheung, P.-Y. Tseng, Y.-L.S. Tsai and T.-C. Yuan, *Global Constraints on Effective Dark Matter Interactions: Relic Density, Direct Detection, Indirect Detection, and Collider*, *JCAP* **05** (2012) 001 [arXiv:1201.3402] [INSPIRE].

[21] M.R. Buckley, *Using Effective Operators to Understand CoGeNT and CDMS-Si Signals*, *Phys. Rev. D* **88** (2013) 055028 [arXiv:1308.4146] [INSPIRE].

[22] M.A. Fedderke, J.-Y. Chen, E.W. Kolb and L.-T. Wang, *The Fermionic Dark Matter Higgs Portal: an effective field theory approach*, *JHEP* **08** (2014) 122 [arXiv:1404.2283] [INSPIRE].

[23] J. Hisano, R. Nagai and N. Nagata, *Effective Theories for Dark Matter Nucleon Scattering*, *JHEP* **05** (2015) 037 [arXiv:1502.02244] [INSPIRE].

[24] S. Bhattacharya and J. Wudka, *Effective theories with dark matter applications*, *Int. J. Mod. Phys. D* **30** (2021) 2130004 [arXiv:2104.01788] [INSPIRE].

[25] D. Barducci, E. Bertuzzo, G.G. di Cortona and G.M. Salla, *Dark photon bounds in the dark EFT*, *JHEP* **12** (2021) 081 [arXiv:2109.04852] [INSPIRE].

[26] P.J. Fox, R. Harnik, J. Kopp and Y. Tsai, *Missing Energy Signatures of Dark Matter at the LHC*, *Phys. Rev. D* **85** (2012) 056011 [arXiv:1109.4398] [INSPIRE].

[27] J. Goodman, M. Ibe, A. Rajaraman, W. Shepherd, T.M.P. Tait and H.-B. Yu, *Constraints on Light Majorana dark Matter from Colliders*, *Phys. Lett. B* **695** (2011) 185 [arXiv:1005.1286] [INSPIRE].

[28] J. Goodman, M. Ibe, A. Rajaraman, W. Shepherd, T.M.P. Tait and H.-B. Yu, *Constraints on Dark Matter from Colliders*, *Phys. Rev. D* **82** (2010) 116010 [arXiv:1008.1783] [INSPIRE].

[29] A. Crivellin and U. Haisch, *Dark matter direct detection constraints from gauge bosons loops*, *Phys. Rev. D* **90** (2014) 115011 [arXiv:1408.5046] [ɪɴSPIRE].

[30] A. Crivellin, U. Haisch and A. Hibbs, *LHC constraints on gauge boson couplings to dark matter*, *Phys. Rev. D* **91** (2015) 074028 [arXiv:1501.00907] [ɪɴSPIRE].

[31] C. Arina, A. Cheek, K. Mimasu and L. Pagani, *Light and Darkness: consistently coupling dark matter to photons via effective operators*, *Eur. Phys. J. C* **81** (2021) 223 [arXiv:2005.12789] [ɪɴSPIRE].

[32] F. Bishara, J. Brod, B. Grinstein and J. Zupan, *Chiral Effective Theory of Dark Matter Direct Detection*, *JCAP* **02** (2017) 009 [arXiv:1611.00368] [ɪɴSPIRE].

[33] A. Crivellin, F. D'Eramo and M. Procura, *New Constraints on Dark Matter Effective Theories from Standard Model Loops*, *Phys. Rev. Lett.* **112** (2014) 191304 [arXiv:1402.1173] [ɪɴSPIRE].

[34] R.J. Hill and M.P. Solon, *Standard Model anatomy of WIMP dark matter direct detection I: weak-scale matching*, *Phys. Rev. D* **91** (2015) 043504 [arXiv:1401.3339] [ɪɴSPIRE].

[35] N.F. Bell, Y. Cai and A.D. Medina, *Co-annihilating Dark Matter: Effective Operator Analysis and Collider Phenomenology*, *Phys. Rev. D* **89** (2014) 115001 [arXiv:1311.6169] [ɪɴSPIRE].

[36] M.J. Baker et al., *The Coannihilation Codex*, *JHEP* **12** (2015) 120 [arXiv:1510.03434] [ɪɴSPIRE].

[37] E. Del Nobile and F. Sannino, *Dark Matter Effective Theory*, *Int. J. Mod. Phys. A* **27** (2012) 1250065 [arXiv:1102.3116] [ɪɴSPIRE].

[38] A. De Simone, A. Monin, A. Thamm and A. Urbano, *On the effective operators for Dark Matter annihilations*, *JCAP* **02** (2013) 039 [arXiv:1301.1486] [ɪɴSPIRE].

[39] S. Matsumoto, S. Mukhopadhyay and Y.-L.S. Tsai, *Effective Theory of WIMP Dark Matter supplemented by Simplified Models: Singlet-like Majorana fermion case*, *Phys. Rev. D* **94** (2016) 065034 [arXiv:1604.02230] [ɪɴSPIRE].

[40] S. Matsumoto, S. Mukhopadhyay and Y.-L.S. Tsai, *Singlet Majorana fermion dark matter: a comprehensive analysis in effective field theory*, *JHEP* **10** (2014) 155 [arXiv:1407.1859] [ɪɴSPIRE].

[41] H. Han, H. Wu and S. Zheng, *Effective field theory of the Majorana dark matter*, *Chin. Phys. C* **43** (2019) 043103 [arXiv:1711.10097] [ɪɴSPIRE].

[42] A. Belyaev et al., *Interplay of the LHC and non-LHC Dark Matter searches in the Effective Field Theory approach*, *Phys. Rev. D* **99** (2019) 015006 [arXiv:1807.03817] [ɪɴSPIRE].

[43] M. Duch, B. Grzadkowski and J. Wudka, *Classification of effective operators for interactions between the Standard Model and dark matter*, *JHEP* **05** (2015) 116 [arXiv:1412.0520] [ɪɴSPIRE].

[44] J. Brod, A. Gootjes-Dreesbach, M. Tammaro and J. Zupan, *Effective Field Theory for Dark Matter Direct Detection up to Dimension Seven*, *JHEP* **10** (2018) 065 [arXiv:1710.10218] [ɪɴSPIRE].

[45] J.C. Criado, A. Djouadi, M. Pérez-Victoria and J. Santiago, *A complete effective field theory for dark matter*, *JHEP* **07** (2021) 081 [arXiv:2104.14443] [ɪɴSPIRE].

[46] B. Grzadkowski, M. Iskrzynski, M. Misiak and J. Rosiek, *Dimension-Six Terms in the Standard Model Lagrangian*, *JHEP* **10** (2010) 085 [arXiv:1008.4884] [INSPIRE].

[47] E.E. Jenkins, A.V. Manohar and P. Stoffer, *Low-Energy Effective Field Theory below the Electroweak Scale: Operators and Matching*, *JHEP* **03** (2018) 016 [arXiv:1709.04486] [INSPIRE].

[48] E.E. Jenkins, A.V. Manohar and P. Stoffer, *Low-Energy Effective Field Theory below the Electroweak Scale: Anomalous Dimensions*, *JHEP* **01** (2018) 084 [arXiv:1711.05270] [INSPIRE].

[49] J.C. Criado, *BasisGen: automatic generation of operator bases*, *Eur. Phys. J. C* **79** (2019) 256 [arXiv:1901.03501] [INSPIRE].

[50] J. Alexander et al., *Dark Sectors 2016 Workshop: Community Report*, (2016) [arXiv:1608.08632] [INSPIRE].

[51] Y. Farzan and A.R. Akbarieh, *Natural explanation for 130 GeV photon line within vector boson dark matter model*, *Phys. Lett. B* **724** (2013) 84 [arXiv:1211.4685] [INSPIRE].

[52] Y. Farzan and A.R. Akbarieh, *Decaying Vector Dark Matter as an Explanation for the 3.5 keV Line from Galaxy Clusters*, *JCAP* **11** (2014) 015 [arXiv:1408.2950] [INSPIRE].

[53] A.V. Manohar, *An Exactly Solvable Model for Dimension Six Higgs Operators and $h \to \gamma\gamma$*, *Phys. Lett. B* **726** (2013) 347 [arXiv:1305.3927] [INSPIRE].

[54] J.R. Ellis, G.B. Gelmini, J.L. Lopez, D.V. Nanopoulos and S. Sarkar, *Astrophysical constraints on massive unstable neutral relic particles*, *Nucl. Phys. B* **373** (1992) 399 [INSPIRE].

[55] R.H. Cyburt, J.R. Ellis, B.D. Fields and K.A. Olive, *Updated nucleosynthesis constraints on unstable relic particles*, *Phys. Rev. D* **67** (2003) 103521 [astro-ph/0211258] [INSPIRE].

[56] M. Kawasaki, K. Kohri, T. Moroi and Y. Takaesu, *Revisiting Big-Bang Nucleosynthesis Constraints on Long-Lived Decaying Particles*, *Phys. Rev. D* **97** (2018) 023502 [arXiv:1709.01211] [INSPIRE].

[57] K.R. Dienes, J. Kumar, P. Stengel and B. Thomas, *Cosmological Constraints on Unstable Particles: Numerical Bounds and Analytic Approximations*, *Phys. Rev. D* **99** (2019) 043513 [arXiv:1810.10587] [INSPIRE].

[58] W. Hu and J. Silk, *Thermalization constraints and spectral distortions for massive unstable relic particles*, *Phys. Rev. Lett.* **70** (1993) 2661 [INSPIRE].

[59] T.R. Slatyer and C.-L. Wu, *General Constraints on Dark Matter Decay from the Cosmic Microwave Background*, *Phys. Rev. D* **95** (2017) 023010 [arXiv:1610.06933] [INSPIRE].

[60] V. Poulin, J. Lesgourgues and P.D. Serpico, *Cosmological constraints on exotic injection of electromagnetic energy*, *JCAP* **03** (2017) 043 [arXiv:1610.10051] [INSPIRE].

[61] ALEPH, DELPHI, L3, OPAL, SLD, LEP ELECTROWEAK WORKING GROUP, SLD ELECTROWEAK GROUP, SLD HEAVY FLAVOUR GROUP collaborations, *Precision electroweak measurements on the Z resonance*, *Phys. Rept.* **427** (2006) 257 [hep-ex/0509008] [INSPIRE].

[62] PLANCK collaboration, *Planck 2018 results. VI. Cosmological parameters*, *Astron. Astrophys.* **641** (2020) A6 [*Erratum ibid.* **652** (2021) C4] [arXiv:1807.06209] [INSPIRE].

[63] L.J. Hall, K. Jedamzik, J. March-Russell and S.M. West, *Freeze-In Production of FIMP Dark Matter*, *JHEP* **03** (2010) 080 [arXiv:0911.1120] [INSPIRE].

[64] F. Elahi, C. Kolda and J. Unwin, *UltraViolet Freeze-in*, *JHEP* **03** (2015) 048 [arXiv:1410.6157] [INSPIRE].

[65] F. D'Eramo, N. Fernandez and S. Profumo, *Dark Matter Freeze-in Production in Fast-Expanding Universes*, *JCAP* **02** (2018) 046 [arXiv:1712.07453] [INSPIRE].

[66] L. Husdal, *On Effective Degrees of Freedom in the Early Universe*, *Galaxies* **4** (2016) 78 [arXiv:1609.04979] [INSPIRE].

[67] PARTICLE DATA GROUP collaboration, *Review of Particle Physics*, *PTEP* **2020** (2020) 083C01 [INSPIRE].

[68] P.F. de Salas, M. Lattanzi, G. Mangano, G. Miele, S. Pastor and O. Pisanti, *Bounds on very low reheating scenarios after Planck*, *Phys. Rev. D* **92** (2015) 123534 [arXiv:1511.00672] [INSPIRE].

[69] I.M. Bloch, A. Caputo, R. Essig, D. Redigolo, M. Sholapurkar and T. Volansky, *Exploring new physics with O(keV) electron recoils in direct detection experiments*, *JHEP* **01** (2021) 178 [arXiv:2006.14521] [INSPIRE].

[70] R. Essig, J. Mardon, M. Papucci, T. Volansky and Y.-M. Zhong, *Constraining Light Dark Matter with Low-Energy e^+e^- Colliders*, *JHEP* **11** (2013) 167 [arXiv:1309.5084] [INSPIRE].

[71] E.E. Jenkins, A.V. Manohar and M. Trott, *Renormalization Group Evolution of the Standard Model Dimension Six Operators I: Formalism and lambda Dependence*, *JHEP* **10** (2013) 087 [arXiv:1308.2627] [INSPIRE].

[72] E.E. Jenkins, A.V. Manohar and M. Trott, *Renormalization Group Evolution of the Standard Model Dimension Six Operators II: Yukawa Dependence*, *JHEP* **01** (2014) 035 [arXiv:1310.4838] [INSPIRE].

[73] R. Alonso, E.E. Jenkins, A.V. Manohar and M. Trott, *Renormalization Group Evolution of the Standard Model Dimension Six Operators III: Gauge Coupling Dependence and Phenomenology*, *JHEP* **04** (2014) 159 [arXiv:1312.2014] [INSPIRE].

[74] F. del Aguila, S. Bar-Shalom, A. Soni and J. Wudka, *Heavy Majorana Neutrinos in the Effective Lagrangian Description: Application to Hadron Colliders*, *Phys. Lett. B* **670** (2009) 399 [arXiv:0806.0876] [INSPIRE].

[75] A. Aparici, K. Kim, A. Santamaria and J. Wudka, *Right-handed neutrino magnetic moments*, *Phys. Rev. D* **80** (2009) 013010 [arXiv:0904.3244] [INSPIRE].

[76] S. Bhattacharya and J. Wudka, *Dimension-seven operators in the standard model with right handed neutrinos*, *Phys. Rev. D* **94** (2016) 055022 [*Erratum ibid.* **95** (2017) 039904] [arXiv:1505.05264] [INSPIRE].

[77] Y. Liao and X.-D. Ma, *Operators up to Dimension Seven in Standard Model Effective Field Theory Extended with Sterile Neutrinos*, *Phys. Rev. D* **96** (2017) 015012 [arXiv:1612.04527] [INSPIRE].

[78] I. Bischer and W. Rodejohann, *General neutrino interactions from an effective field theory perspective*, *Nucl. Phys. B* **947** (2019) 114746 [arXiv:1905.08699] [INSPIRE].

[79] J. Alcaide, S. Banerjee, M. Chala and A. Titov, *Probes of the Standard Model effective field theory extended with a right-handed neutrino*, *JHEP* **08** (2019) 031 [arXiv:1905.11375] [INSPIRE].

[80] A. Datta, J. Kumar, H. Liu and D. Marfatia, *Anomalous dimensions from gauge couplings in SMEFT with right-handed neutrinos*, *JHEP* **02** (2021) 015 [`arXiv:2010.12109`] [ɪɴSPIRE].

[81] M. Chala and A. Titov, *One-loop running of dimension-six Higgs-neutrino operators and implications of a large neutrino dipole moment*, *JHEP* **09** (2020) 188 [`arXiv:2006.14596`] [ɪɴSPIRE].

[82] T. Han, J. Liao, H. Liu and D. Marfatia, *Scalar and tensor neutrino interactions*, *JHEP* **07** (2020) 207 [`arXiv:2004.13869`] [ɪɴSPIRE].

[83] A. Datta, J. Kumar, H. Liu and D. Marfatia, *Anomalous dimensions from Yukawa couplings in SMNEFT: four-fermion operators*, *JHEP* **05** (2021) 037 [`arXiv:2103.04441`] [ɪɴSPIRE].